Synthesis and Reactivity of *σ*-Alkynyl/*P*-Bonded Phosphinoalkyne Platinum Complexes toward *cis*-[M(C_6F_5)$_2$(thf)$_2$] (M = Pt, Pd)†

Irene Ara,‡ Larry R. Falvello,‡ Susana Fernández,§ Juan Forniés,*,‡ Elena Lalinde,*,§ Antonio Martín,‡ and M. Teresa Moreno‡

Departamento de Química Inorgánica, Instituto de Ciencia de Materiales de Aragón, Universidad de Zaragoza-Consejo Superior de Investigaciones Científicas, 50009 Zaragoza, Spain, and Departamento de Química, Universidad de La Rioja, 26001 Logroño, Spain

Received July 31, 1997⊗

The reactivity of *cis*-bis(alkynyl)bis((diphenylphosphino)alkyne)platinum(II) complexes *cis*-[Pt(C≡CR)$_2$L$_2$] (R = Ph, Bu^t; L = PPh$_2$C≡CPh (L^1), PPh$_2$C≡CBu^t (L^2); **1**−**4**), formed by displacement of the COD ligand from [Pt(C≡CR)$_2$(COD)], toward *cis*-[M(C_6F_5)$_2$(thf)$_2$] (M = Pt, Pd, thf = tetrahydrofuran; in both a 1:1 and 1:2 molar ratio) has been investigated. Treatment of **1**−**4** with 1 equiv of *cis*-[M(C_6F_5)$_2$(thf)$_2$] affords dinuclear derivatives [{L$_2$Pt-(μ-η^1:η^2-C≡CR)$_2$}M(C_6F_5)$_2$] (**5**−**12**) with exclusive formation of doubly alkynyl-bridged systems. The molecular structure of [{(Bu^{t}C≡CPh$_2$P)$_2$Pt(μ-η^1:η^2-C≡CPh)$_2$}Pd(C_6F_5)$_2$], **10**, is presented. In contrast, it was found that the course of the reactions with 2 equiv of *cis*-[M(C_6F_5)$_2$(thf)$_2$] strongly depend on the alkynyl substituents and metal centers. Thus, treatment of *tert*-butylalkynyl derivatives *cis*-[Pt(C≡CBu^t)$_2$L$_2$] (**2**, **4**) with 2 equiv of *cis*-[M(C_6F_5)$_2$(thf)$_2$] (M = Pt, Pd) only gives the expected trinuclear complexes **15A** and **18A**, in the case of the reactions with *cis*-[Pt(C_6F_5)$_2$(thf)$_2$]. The molecular structure of the complex [{Pt(μ-κ(*P*):η^2-PPh$_2$C≡CPh)$_2$(μ-η^1:η^2-C≡CBu^t)$_2$}{Pt(C_6F_5)$_2$}$_2$], **15A**, reveals that both the complexed *cis*-Pt(C_6F_5)$_2$ moieties are symmetrically linked to the precursor "*cis*-[Pt(C≡CBu^t)$_2$-(PPh$_2$C≡CPh)$_2$]", with the platinum atoms connected by two unusual mixed alkynyl/phosphinoalkyne bridging systems. On the other hand, similar reactions of phenylethynyl derivatives (**1**, **3**) with 2 equiv of *cis*-[Pd(C_6F_5)$_2$(thf)$_2$] and **3** (L = PPh$_2$C≡CBu^t) with *cis*-[Pt-(C_6F_5)$_2$(thf)$_2$] lead, instead, to the unexpected trinuclear PtPd$_2$ (**14B**, **17B**) and Pt$_3$ (**16B**) derivatives which display terminal phosphinoalkyne ligands and, hence, contain the alkynyl groups acting as μ_3-η^2 (*σ*-Pt edge Pd or Pt) bridging ligands. However, a mixture of both types of isomers **13A** and **13B** (50:32) is observed in the reaction system *cis*-[Pt(C≡CPh)$_2$-(PPh$_2$C≡CPh)$_2$] (**1**)/*cis*-[Pt(C_6F_5)$_2$(thf)$_2$]. The following order of bonding capability is deduced from this study: alkynyl > *P*-bonded phosphinoalkyne and XC≡CPh fragments > XC≡CBu^t (X = Pt, P).

Introduction

Phosphinoalkynes and acetylides have been widely used in the formation of organometallic complexes containing two or more transition metals. Phosphinoalkynes (PPh$_2$C≡CR) are potentially difunctional ligands with the capacity to coordinate as simple phosphines[1] or disubstituted acetylenes[2] or to simultaneously use the phosphorus lone pair and the acetylenic π-orbitals in a polydentate bonding mode.[3] Although all three of these possibilities have been observed, it seems that the coordinating ability of PPh$_2$C≡CR is usually dominated by the phosphine donor sites, especially for complexes of metals in their normal oxidation states. The participation of the acetylenic triple bonds in coordination seems to require a low-valent metal site with a high affinity for alkyne π-electrons.[2,3] These bonding situations are well represented by the low-valent dinuclear complexes [Fe$_2$(μ-η^3-PPh$_2$C≡CPh)$_2$(CO)$_6$],[3c] [Ni$_2$(μ-η^3-PPh$_2$C≡CBu^t)$_2$(CO)$_2$],[3f] [M$_2$(μ-η^3-PPh$_2$C≡CPh)$_2$(PPh$_3$)$_2$] (M = Pt, Pd)[3g] (Scheme 1, **A**), and [Fe$_2$(μ-η^3-PPh$_2$C≡CBu^t)(CO)$_8$][3d] (Scheme 1, **B**), in which the PPh$_2$C≡CR groups act as four-electron bridging ligands (*P*, η^2) and by the tetranuclear [Co$_4$(μ_3-η^3-PPh$_2$C≡CR)$_2$(CO)$_{10}$][3a] and trinuclear [Ni$_2$Cp$_2$(μ_3-η^3-PPh$_2$C≡CPh)Ni(CO)$_3$][2b] derivatives in which the ligands behave as six-electron donors (*P*, η^2:η^2, Scheme 1, **C**). In this context, we have recently shown that the reaction of *cis*-[MCl$_2$(PPh$_2$C≡CPh)$_2$] (M = Pt, Pd) with *cis*-[Pt(C_6F_5)$_2$(thf)$_2$] gives the unusual dinuclear derivatives [(C_6F_5)$_2$Pt(μ-Cl)(μ-η^3-PPh$_2$C≡CPh)-MCl(PPh$_2$C≡CPh)][4] (Scheme 1, **D**) containing a diphen-

† Dedicated to Prof. Pascual Royo on the occasion of his 60th birthday.

‡ Universidad de Zaragoza.

§ Universidad de La Rioja.

⊗ Abstract published in *Advance ACS Abstracts*, December 1, 1997.

(1) (a) Sappa, E.; Valle, M.; Predieri, G.; Tiripicchio, A. *Inorg. Chim. Acta* **1984**, *88*, L23. (b) Wong, Y. S.; Jacobson, S. E.; Chieh, P. C.; Carty, A. J. *Inorg. Chem.* **1974**, *13*, 284. (c) Berau, G.; Carty, A. J.; Chieh, P. C.; Patel, H. A. *J. Chem. Soc., Dalton Trans.* **1973**, 488.

(2) (a) Patel, H. A.; Carty, A. J.; Hota, N. K. *J. Organomet. Chem.* **1973**, *50*, 247. (b) Carty, A. J.; Paik, H. N.; Ng, T. W. *J. Organomet. Chem.* **1974**, *74*, 279.

(3) (a) Hota, N. K.; Patel, H. A.; Carty, A. J.; Mathew, M.; Palenik, G. J. *J. Organomet. Chem.* **1971**, *32*, C55. (b) Sappa, E.; Predieri, G.; Tiripicchio, A.; Tiripicchio-Camelini, M. *J. Organomet. Chem.* **1985**, *297*, 103. (c) Carty, A. J.; Paik, H. N.; Palenik, G. J. *Inorg. Chem.* **1977**, *16*, 300. (d) Carty, A. J.: Smith, W. F.; Taylor, N. J. *J. Organomet. Chem.* **1978**, *146*, C1. (e) O'Connor, T.; Carty, A. J.; Mathew, M.; Palenik, G. J. *J. Organomet. Chem.* **1972**, *38*, C15. (f) Carty, A. J.; Dymock, K.; Paik, H. N.; Palenik, G. J. *J. Organomet. Chem.* **1974**, *70*, C17. (g) Jacobsen, S.; Carty, A. J.; Mathew, M.; Palenik, G. J. *J. Am. Chem. Soc.* **1974**, *96*, 4330.

S0276-7333(97)00663-8 CCC: $14.00

Scheme 1

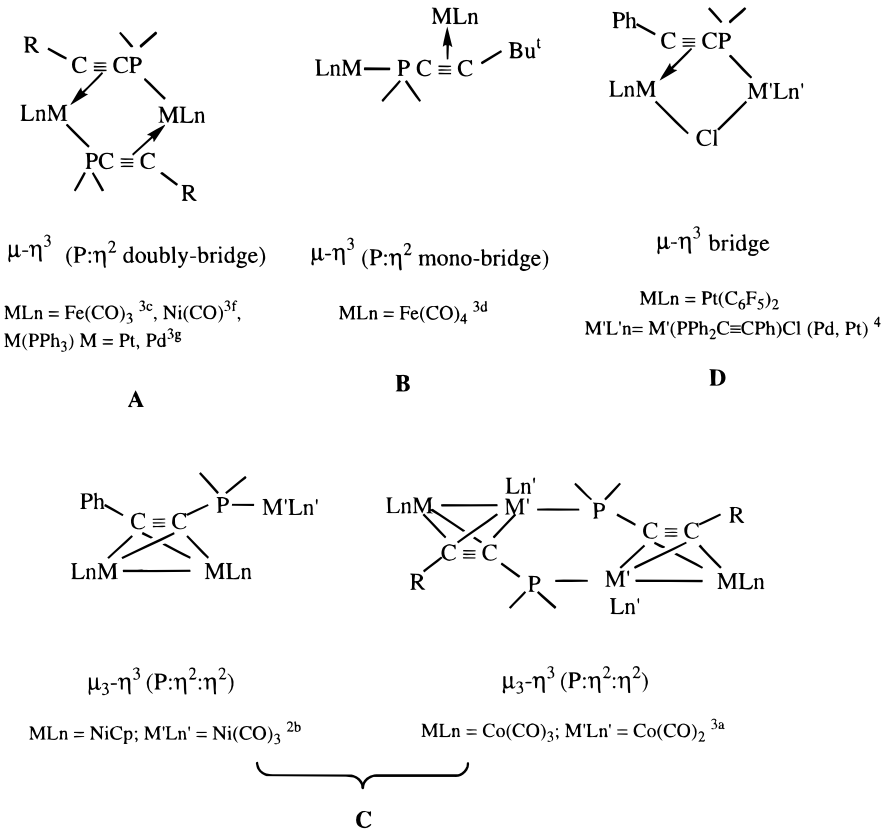

yl(phenylethynyl)phosphine acting as a bridging ligand (μ-*P*:η^2) between two Pt(II) centers. The formation of these derivatives is rather surprising since the isomeric dinuclear doubly bridging chloride complexes [$(C_6F_5)_2$-Pt(μ-Cl)$_2$M($PPh_2C{\equiv}CPh)_2$] would have been expected. Interestingly, we observed that these complexes **D**, which are sparingly soluble in common organic solvents, dissolve in CD_2Cl_2, yielding a mixture of the isomers **D** along with the expected M(μ-Cl)$_2$Pt derivatives. This fact suggests that in solution the migration of the Pt-$(C_6F_5)_2$ unit around the *cis*-$PtCl_2(PPh_2C{\equiv}CPh)_2$ fragment [μ-Cl, $\kappa(P)$:η^2] → (μ-Cl)$_2$ probably has a small energetic cost and that steric effects involving the two mutually *cis* bulky $PPh_2C{\equiv}CPh$ groups should account in part for the μ-η^3-$PPh_2C{\equiv}CPh$ bridging preference in the solid phase.

On the other hand, the ability of alkynyl ligands to bind several metal centers through σ and π bonds is now firmly established.[5] In particular, we have recently found that either neutral or anionic alkynylplatinum substrates $[L_nM(C{\equiv}CR)_2]^{n-}$ (n = 0, L = phosphine, COD; n = 2, L = C_6F_5, C≡CR) react with Lewis-acidic metal complexes yielding homo- and hetero- di- and trinuclear compounds stabilized with double alkynyl bridges, Pt(μ-C≡CR)$_2$M.[5a,6]

In this paper, we report on the synthesis of neutral *cis*-bis(alkynyl)bis((diphenylphosphino)alkyne)platinum-(II) complexes *cis*-[Pt(C≡CR)$_2$L$_2$] (R = Ph, Bu^t; L = $PPh_2C{\equiv}CPh$, $PPh_2C{\equiv}CBu^t$) and describe their reactivity toward *cis*-[M$(C_6F_5)_2$(thf)$_2$] (M = Pt, Pd) in either a 1:1 or 1:2 molar ratio. The syntheses of both di- and trinuclear complexes and the solid-state structures of [{($Bu^tC{\equiv}CPh_2P)_2$Pt(μ-η^1:η^2-C≡CPh)$_2$}Pd$(C_6F_5)_2$], **10**, an unusual triplatinum [{Pt(μ-κ(*P*):η^2-$PPh_2C{\equiv}CPh)_2$(μ-η^1:η^2-C≡CBu^t)$_2$}{Pt$(C_6F_5)_2$}$_2$], **15A**, and an unprecedented triangular trimetallic bicapped [{$(PPh_2C{\equiv}CBu^t)_2$Pt(μ_3-η^2-C≡CPh)$_2$}{Pt$(C_6F_5)_2$}$_2$] complex, **16B**, are presented.

Results and Discussion

Syntheses of *cis*-[Pt(C≡CR)$_2$L$_2$] Complexes. A series of stable mononuclear σ-alkynyl/*P*-coordinated (diphenylphosphino)alkyne complexes *cis*-[Pt(C≡CR)$_2$L$_2$] (R = Ph or Bu^t; L = $PPh_2C{\equiv}CPh$ (L^1), $PPh_2C{\equiv}CBu^t$ (L^2); **1**−**4**) are easily prepared in high yield by displacement of the weakly coordinating COD ligand from [Pt-(C≡CR)$_2$COD] (R = Ph, Bu^t) derivatives by the appropriate diphenylalkynylphosphine ligands (eq 1). They are isolated as white solids, and their spectroscopic data (Tables 1 and 2) unequivocally confirm the *P*-coordination mode of the difunctional $PPh_2C{\equiv}CR$

(4) Forniés, J.; Lalinde, E.; Martín, A.; Moreno, M. T.; Welch, A. J. *J. Chem. Soc., Dalton Trans.* **1995**, 1333.

(5) (a) Forniés, J.; Lalinde, E. *J. Chem. Soc., Dalton Trans.* **1996**, 2587. (b) Beck, W.; Niemer, B.; Wieser, M. *Angew. Chem., Int. Ed. Engl.* **1993**, *32*, 923. (c) Lotz, S.; Van Rooyen, P. H.; Meyer, R. *Adv. Organomet. Chem.* **1995**, *37*, 219 and references therein. (c) Nast, R. *Coord. Chem. Rev.* **1982**, *47*, 89. (d) Carty, A. J. *Pure Appl. Chem.* **1982**, *54*, 113. (e) Bruce, M. I. *Pure Appl. Chem.* **1986**, *58*, 553; **1990**, *6*, 1021. (f) Raithby, P. R.; Rosales, M. J. *Adv. Inorg. Chem. Radiochem.* **1985**, *29*, 169. (g) Sappa, E.; Tiripicchio, A.; Braunstein, P. *Coord. Chem. Rev.* **1985**, *65*, 219. (h) Bruce. M. I. *Chem. Rev.* **1991**, *91*, 197. (i) Davies, S. G.; McNally, J. P.; Smallridge, A. J. *Adv. Organomet. Chem.* **1990**, *30*, 1. (j) Pavan Kumar, P. N. V.; Jemmis, E. D. *J. Am. Chem. Soc.* **1988**, *110*, 125. (k) Jeannin, Y. *Transition Met. Chem.* **1993**, *18*, 122. (l) Cauletti, C.; Furlani, C.; Sebald, A. *Gazz. Chim. Ital.* **1988**, *118*, 1.

(6) (a) Forniés, J.; Gómez-Saso, M. A.; Lalinde, E.; Martínez, F.; Moreno, M. T. *Organometallics* **1992**, *11*, 2873. (b) Forniés, J.; Lalinde, E.; Martín, A.; Moreno, M. T. *J. Chem. Soc., Dalton Trans.* **1994**, 135. (c) Berenguer, J. R.; Forniés, J.; Lalinde, E.; Martínez, F. *J. Organomet. Chem.* **1994**, *470*, C15. (d) Berenguer, J. R.; Forniés, J.; Lalinde, E.; Martínez, F. *J. Chem. Soc., Chem. Commun.* **1995**, 1227. (e) Forniés, J.; Lalinde, E.; Martín, A.; Moreno, M. T. *J. Organomet. Chem.* **1995**, *490*, 179.

Published on December 23, 1997 on http://pubs.acs.org | doi: 10.1021/om970663y

Table 1. Elemental Analyses, Yield, Relevant IR Absorption and Mass Spectral Data for the Complexes[a]

compound	analysis (%)[b] C	analysis (%)[b] H	yield (%)	IR (cm^{-1}) ν(C≡C)	IR (cm^{-1}) $\nu(C_6F_5)$X-sen s[c]	mass spectra m/z[d]
1 $[Pt(C{\equiv}CPh)_2(L^1)_2]$	68.82 (69.34)	4.20 (4.16)	82	2173 (vs) 2124(m)		1155 ($[M + PPh_2]^+$, 19), 970 ($[M]^+$, 15), 868 ($[M - C{\equiv}CPh]^+$, 14), 767 ($[Pt(PPh_2C{\equiv}CPh)_2]^+$, 100), 377 ($[Pt(PPh_2)]^+ - 2$, 42)
2 $[Pt(C{\equiv}CBu^t)_2(L^1)_2]$	66.52 (67.16)	5.15 (5.20)	78	2178 (vs)		930 ($[M]^+$, 25), 848 ($[M - C{\equiv}CBu^t]^+$, 12), 767 $[(Pt(PPh_2C{\equiv}CPh)_2]^+$, 100), 378 ($[Pt(PPh_2)]^+ - 1$, 22)
3 $[Pt(C{\equiv}CPh)_2(L^2)_2]$	66.72 (67.16)	4.91 (5.20)	92	2203 (w), 2162 (m), 2117 (m)		930 ($[M]^+$, 25), 828 ($[M - C{\equiv}CPh]^+$, 8), 727 ($[Pt(PPh_2C{\equiv}CBu^t)_2]^+$, 100), 379 ($[Pt(PPh_2)]^+$, 39)
4 $[Pt(C{\equiv}CBu^t)_2(L^2)_2]$	64.17 (64.78)	6.22 (6.34)	94	2208 (m), 2167 (s), 2131(vw)		890 ($[M]^+$, 10), 808 ($[M - C{\equiv}CBu^t]^+$, 9), 727 ($[Pt(PPh_2C{\equiv}CBu^t)_2]^+$, 100), 379 ($[Pt(PPh_2)]^+$, 22)
5 $[\{L^1{}_2Pt(\mu\text{-}\eta^1{:}\eta^2\text{-}C{\equiv}CPh)_2\}Pt(C_6F_5)_2]$	53.92 (54.48)	2.88 (2.69)	51	2175 (vs)	801(vs), 791 (s)	1499 ($[M]^+$, 8), 1332 ($[M - C_6F_5]^+$, 8), 1296($[M - 2C{\equiv}CPh]^+$, 11), 767 ($[Pt(PPh_2C{\equiv}CPh)_2]^+$, 29)
6 $[\{L^1{}_2Pt(\mu\text{-}\eta^1{:}\eta^2\text{-}C{\equiv}CPh)_2\}Pd(C_6F_5)_2]$	57.78 (58.19)	2.95 (2.87)	57	2178 (vs), 2068 (w)	789 (m), 779 (m)	973 ($[PtPd(PPh_2C{\equiv}CPh)_2(C{\equiv}CPh)]^+$, 20), 873 ($[PtPd(PPh_2C{\equiv}CPh)_2]^+$, 75), 767 ($[Pt(PPh_2C{\equiv}CPh)_2]^+$, 40)
7 $[\{L^1{}_2Pt(\mu\text{-}\eta^1{:}\eta^2\text{-}C{\equiv}CBu^t)_2\}Pt(C_6F_5)_2]$	52.70 (52.68)	3.82 (3.31)	85	2178 (vs), 2040 (vw)	801 (vs), 788 (s)	1458 ($[M]^+$, 15), 1296 ($[Pt_2(PPh_2C{\equiv}CPh)_2(C_6F_5)_2]^+$, 30), 1129 ($[Pt_2(PPh_2C{\equiv}CPh)_2(C_6F_5)]^+$, 54), 1028 ($[Pt_2(PPh_2C{\equiv}CPh)(PPh_2)(C_6F_5)]^+$, 80), 767 ($[Pt(PPh_2C{\equiv}CPh)_2]^+$, 65), 377 ($[Pt(PPh_2)]^+ - 2$, 65)
8 $[\{L^1{}_2Pt(\mu\text{-}\eta^1{:}\eta^2\text{-}C{\equiv}CBu^t)_2\}Pd(C_6F_5)_2]$	55.70 (56.09)	4.02 (3.53)	93	2179 (vs), 2061 (w), 2044 (w)	788 (s), 775 (s)	1372 ($[M]^+$, 5), 874 ($[PtPd(PPh_2C{\equiv}CPh)_2]^+$, 100), 767 ($[Pt(PPh_2C{\equiv}CPh)_2]^+$, 20)
9 $[\{L^2{}_2Pt(\mu\text{-}\eta^1{:}\eta^2\text{-}C{\equiv}CPh)_2\}Pt(C_6F_5)_2]$	52.13 (52.68)	3.68 (3.31)	65	2200 (m, br), 2172 (s), 2159 (s)	804 (s), 793 (s)	1458 ($[M]^+$, 5), 1089 ($[Pt_2(PPh_2C{\equiv}CBu^t)_2(C_6F_5)]^+$, 50), 727 $[Pt(PPh_2C{\equiv}CBu^t)_2]^+$, 86), 379 ($[Pt(PPh_2)]^+$, 80)
10 $[\{L^2{}_2Pt(\mu\text{-}\eta^1{:}\eta^2\text{-}C{\equiv}CPh)_2\}Pd(C_6F_5)_2]$	53.50 (53.33)	3.66 (3.35)	70	2212 (s), 2169 (s)	792 (s), 779 (s)	1371 ($[M]^+$, 15), 834 ($[PtPd(PPh_2C{\equiv}CBu^t)_2]^+$, 100), 767 ($[Pt(PPh_2C{\equiv}CPh)_2]^+$, 50), 379 ($[Pt(PPh_2)]^+$, 43)
11 $[\{L^2{}_2Pt(\mu\text{-}\eta^1{:}\eta^2\text{-}C{\equiv}CBu^t)_2\}Pt(C_6F_5)_2]$	50.63 (53.78)	3.44 (3.26)	68	2210 (s), 2168 (s)	*e*	1419 ($[M]^+$, 3), 727 ($[Pt(PPh_2C{\equiv}CBu^t)_2]^+$, 100), 379 ($[Pt(PPh_2)]^+$, 54)
12 $[\{L^2{}_2Pt(\mu\text{-}\eta^1{:}\eta^2\text{-}C{\equiv}CBu^t)_2\}Pd(C_6F_5)_2]$	53.66 (54.17)	4.01 (4.24)	51	2210 (m), 2170 (s), 2062 (w), 2041 (w)	780 (s), 775 (sh)	1331 ($[M]^+$, 3), 832 ($[PtPd(PPh_2C{\equiv}CBu^t)_2]^+$, 51), 727 ($[Pt(PPh_2C{\equiv}CBu^t)_2]^+$, 32), 379 ($[Pt(PPh_2)]^+$, 23)
14B $[\{L^1{}_2Pt(\mu_3\text{-}\eta^2\text{-}C{\equiv}CPh)_2)\}\{Pd(C_6F_5)_2\}_2]$	51.02 (51.91)	1.69 (2.18)	70	2179 (s), 2151 (w), 1951 (w)	794 (s), 780 (s)	973 ($[PtPd(PPh_2C{\equiv}CPh)_2(C{\equiv}CPh)^+$, 15), 872 ($[PtPd(PPh_2C{\equiv}CPh)_2]^+$, 100), 767 $[Pt(PPh_2C{\equiv}CPh)_2]^+$, 48)
15A $[\{cis\text{-}Pt(\mu\text{-}\kappa(P){:}\text{-}\eta^2\text{-}L^1)_2(\mu\text{-}\eta^1{:}\eta^2C{\equiv}CBu^t)_2\}\{Pt(C_6F_5)_2\}_2]$	46.45 (45.91)	2.35 (2.43)	86	2064 (m), 2028 (m), 1980 (m)	803 (vs), 792 (s)	1458 ([**7**]$^+$, 7), 1128 ($[Pt_2(PPh_2C{\equiv}CPh)_2(C_6F_5)_2]^+$, 33), 727 ($[Pt(PPh_2C{\equiv}CBu^t)_2]^+$, 30), 377 ($[Pt(PPh_2)]^+ - 2$, 52)
16B $[\{L^2{}_2Pt(\mu_3\text{-}\eta^2\text{-}C{\equiv}CPh)_2\}\{Pt(C_6F_5)_2\}_2]$	46.64 (45.91)	2.03 (2.43)	45	2210 (w), 2169 (m), 1883 (w), 1870 (sh)	804 (vs), 798 (s)	1090 ($[Pt_2(PPh_2C{\equiv}CBu^t)_2(C_6F_5)]^+ + 1$, 32), 726 ($[Pt(PPh_2C{\equiv}CBu^t)_2]^+ - 1$, 48), 459 ($[Pt(PPh_2C{\equiv}CBu^t)]^+$, 54), 379 ($[Pt(PPh_2)]^+$, 100)
17B $[\{L^2{}_2Pt(\mu_3\text{-}\eta^2\text{-}C{\equiv}CPh)_2)\}\{Pd(C_6F_5)_2\}_2]$	49.92 (50.41)	2.31 (2.67)	40	2210 (s), 2169 (s), 1951 (d)	792 (s), 780 (s)	832 ($[PtPd(PPh_2C{\equiv}CBu^t)_2]^+ - 1$, 58), 727 ($[Pt(PPh_2C{\equiv}CBu^t)_2]^+$, 42), 379 ($[Pt(PPh_2)]^+$, 100)
18A $[\{cis\text{-}Pt(\mu\text{-}\kappa(P){:}\text{-}\eta^2\text{-}L^2)_2(\mu\text{-}\eta^1{:}\eta^2C{\equiv}CBu^t)_2\}\{Pt(C_6F_5)_2\}_2]$	43.85 (44.38)	2.52 (2.90)	57	2017 (m), 1991 (sh)	802 (vs), 790 (s)	1417 ([**11** - 2]$^+$, 5), 1089 ($[Pt_2(PPh_2C{\equiv}CBu^t)_2(C_6F_5)]^+$, 53), 1008 ($[Pt_2(PPh_2C{\equiv}CBu^t)(PPh_2)(C_6F_5)]^+$, 27), 727 ($[Pt(PPh_2C{\equiv}CBu^t)_2]^+$, 100), 379 ($[Pt(PPh_2)]^+$, 100)

[a] L = $PPh_2C{\equiv}CPh$ (L^1), $PPh_2C{\equiv}CBu^t$ (L^2). [b] Calculated values in parentheses. [c] X-sensitive mode of the C_6F_5 groups. [d] FAB^+ spectrum. [e] The expected $\nu(C_6F_5)$X-sens absorptions cannot be unambigously assigned.

Table 2. ^{19}F, ^{31}P, and ^{1}H NMR Data[a] for the Complexes

		^{19}F			^{31}P		^{1}H	
compound	T[a]	F_o[b]	F_p	F_m	$\delta(P)$	$^{1}J_{^{195}Pt-^{31}P}$	δ(Ph)	δ(Bu^t)
1					−5.87	2343	7.87 (m, 8H); 7.30 (m, 12H); 7.17 (m, 6H); 6.99 (m, 8H); 6.89 (m, 6H)	
2					−6.13	2311	7.83 (m, 10H); 7.30 (m); 7.15 (m); 6.98 (m, 20H)	0.90 (s, 18H)
3					−7.90	2360	7.80 (m, 8H); 7.33 (m); 7.00 (m); 6.88 (m, 22H)	0.97 (s, 18H)
4					−7.76	2335	7.76 (m, 10H); 7.31 (m, 20H)	0.97 (s, 18H), 0.88 (s, 18H)
5	20	−117.3 (s) [406], −116.5 (s, br) [∼310]	−164.4 (t)	−166.4 (m), −165.1 (s, br)	−10.40	2679	7.90 (m, 8H); 7.37 (m, 12H); 7.21 (m, 8H); 7.03 (m, 8H); 6.86 (d, 4H)	
	−50	−118.3 (s, br) [461]	−163.2 (t)	−165.9 (s, br)				
6[c]	20	−114.7 (d)	−163.3 (t)	−165.5 (m)	−8.53	2644	7.89 (m, 8H); 7.36 (m, 12H); 7.19 (m, 8H); 7.02 (m, 8H); 6.70 (d, 4H)	
7		−114.8 (m) [393], −116.3 (s) [458]	−164.7 (t)	−165.9 (m, br), −166.5 (m)	−10.56	2674	7.85 (m, 8H); 7.33 (m, 12H); 7.18 (m, 6H); 7.00 (m, 4H)	0.78 (s, 18H)
8		−111.4 (d), −112.2 (m)	−162.9 (t)	−164.9 (m), −165.2 (m)	−8.90	2661	7.86 (m, 8H); 7.33 (m, 12H); 7.20 (m, 6H); 7.01 (d, 4H)	0.78 (s, 18H)
9	20	−117.0 (d) [410]	−164.3 (t)	−166.2 (m)	−12.79	2692	7.84 (m, 8H); 7.42 (m, 12H); 7.15 (m, 2H); 7.03 (m, 4H); 6.83 (d, 4H)	1.03 (s, 18H)
	−50	−117.0 (br), −118.0 (br)	−163.2 (t)	−165.3 (br), −165.9 (br)				
10[c]	20	−114.3 (d)	−163.1 (t)	−165.3 (m)	−10.78	2656	7.81 (m, 8H); 7.40 (m, 12H); 7.13 (m, 2H); 6.99 (m, 4H); 6.66 (d, 4H)	1.03 (s, 18H)
11		−114.7 (s) [402], −115.8 (d) [442]	−164.7 (t)	−165.8 (s), −166.2 (s)	−13.06	2689	7.78 (m, 8H); 7.38 (s, 12H)	0.99 (s, 18H), 0.76 (s, 18H)
12		−111.1 (d), −112.3 (m)	−163.2 (t)	−165.2 (m)	−10.90	2674	7.77 (s, br, 8H); 7.36 (s, br, 12H)	1.00 (s, 18H), 0.76 (s, 18H)
14B[d]	20	−113.1 (br)	−160.5 (t)	−164.0 (m)	−14.10	2891	7.97 (m, 6H); 7.27 (s, 24H); 6.93 (m, 8H)	
	−50	−112.6 (s, br), −114.1 (d)	−159.9 (t)	−162.8 (s), −164.6 (m)				
15A[d]	20	−114.6 (d) [367], −115.3 (s, br) (−116.8) (br, $\Delta\nu \approx 515$)	−161.3 (t), −161.5 (t)	−163.5 (m, 1F), −164.3 (m, 1F), −164.1 (br, 2F)	−0.92	2488	7.91 (m, 4H); 7.53 (m, 12H); 7.33−7.18 (m, 12H); 7.00 (m, 4H)	0.9 (s, 18H)
	−50	−114.8 (md) [384], −115.5 (m), −116.3 (m) [∼274], −118.3 (dm) [347]	−160.75 (t), −160.9 (t)	−162.7 (m, 2F_m), −163.2 (m, 2F_m), −163.8 (m, 4F_m)				
16B[d]	20	−116.1 (br)	−161.7 (t)	−165.0 (s, br)	−20.55	3008	7.96 (m, 6H); 7.43 (m, 12H); 7.15 (m, 4H); 6.91 (m, 4H); 6.82 (m, 4H)	1.14 (s, 18H)
	−50	−115.1 (s),[e] −118.2 (d)	−161.0 (t)	−163.9 (m), −165.1 (m)				
17B[d]	20	−113.1 (br)	−160.7 (t)	−164.0 (m)	−14.80	2910	7.92 (m, 2H); 7.39 (m, 6H); 6.93 (m, 2H)	1.1 (s, 18H)
	−50	−112.7 (s, br), −114.0 (d)	−160.0 (t)	−162.9 (s), −164.1 (m)				
18A	20	−115.1 (br),[e] −116. 1 (br)	−161.1 (t), −161.7 (t)	−163.9 (br), −164.4 (br)	−1.96	2501	7.87 (m, 4H); 7.52 (m, 6H); 7.36 (m, 6H); 7.06 (m, 4H)	1.16 (s, 18H), 0.94 (s, 18H)
	−50	−115.1 (m, 4F_o), −116.1 (m, 2F_o), −117.7 (m, 2F_o)	−160.3[f] (br, 2F_p), −161.3[f] (br, 2F_p)	−162.8 (m, br, 4F_m), −163.8 (m, br, 4F_m)				

[a] In $CDCl_3$ at 20 °C, chemical shifts are reported relative to $CFCl_3$, H_3PO_4 (85%), and $SiMe_3$ (as external references). [b] $^{3}J_{^{195}Pt-F_o}$ in brackets. [c] The same spectral pattern was observed at −50 °C. [d] Coalescence temperature, **14B** (∼278 K), **15A** (∼288 K), **16B** (∼263 K), **17B** (∼275 K). [e] Pt satellites are seen, but the $^{3}J_{Pt-F_o}$ cannot be unambigously determined. [f] Overlapping of two triplets.

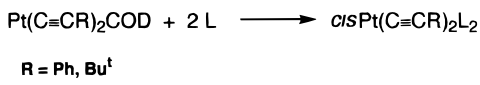

(1)

R	L	
Ph	$PPh_2C{\equiv}CPh$	**1**
Bu^t	$PPh_2C{\equiv}CPh$	**2**
Ph	$PPh_2C{\equiv}CBu^t$	**3**
Bu^t	$PPh_2C{\equiv}CBu^t$	**4**

ligands: (i) the presence of strong absorptions (one for **1** and **2** or two for **3** and **4**) in the 2167−2208 cm^{-1} region due to the ν(C≡C) of the phosphinoalkyne ligands shows that these groups are acting as *P*-donors. Complexes **1**, **3**, and **4** display additional absorptions of medium intensity in the 2117−2131 cm^{-1} region attributed to the ν(C≡C) of terminal alkynyl ligands. (ii) The presence of a singlet in the $^{31}P\{^1H\}$ NMR (δ −5.87, −7.90), especially the magnitude of $^1J_{^{195}Pt-^{31}P}$ (2311−2360 Hz) which is comparable to that reported for mononuclear platinum complexes having a tertiary phosphine *trans* to a terminal alkynide group, is consistent with a *cis* configuration of the ligands about platinum.[6,7] In the ^{13}C NMR spectra, the acetylenic carbons (see Table 3 and Experimental Section for details) are found in the typical chemical shift ranges (C_α/C_β, $Pt-C_\alpha{\equiv}C_\beta-R$ 84.7−102.3/108.8−117 ppm; $P-C_\alpha{\equiv}C_\beta-R$ 70.7/118.3 ppm). The C_α signals are observed as a first-order doublet of doublets ($Pt-C_\alpha$) or as a doublet ($P-C_\alpha$, dd for **1** and **2**), while the alkyne C_β resonances exhibit the typical A part of a second-order AXX′ system. The two alkynyl ($Pt-C_\alpha{\equiv}C_\beta R$) carbon signals could be easily identified due to their significantly different coupling constants to the ^{195}Pt nuclei. The magnitude of the coupling constants $^{13}C-^{195}Pt$ ($^1J_{C-Pt}$ = 1135−1150 Hz, $^2J_{C-Pt}$ = 309−314 Hz) are comparable to those observed in similar neutral bis(alkynyl) complexes of the type $[Pt(C{\equiv}CR)_2L_2]$ (L = phosphine)[8] but, as expected, are notably larger than those observed by us in the anionic derivatives $[Pt(C{\equiv}CR)_2X_2]^{2-}$ (X = C≡CR or C_6F_5) (924−1048)/250−293 Hz $^1J_{C-Pt}/^2J_{C-Pt}$).[9] Although all complexes (**1**−**4**) exhibit signals due to the molecular peaks in the FAB(+) mass spectra, the most intense peaks correspond to the loss of the two alkynyl groups $[PtL_2]^+$ (100), and the peaks assignable to the loss of one alkynyl ligand $[Pt(C{\equiv}CR)L_2]^+$ are also present.

Syntheses of Dinuclear Complexes. In order to develop the synthetic potential of these *σ*-bonded species *cis*-$[Pt(C{\equiv}CR)_2L_2]$, we have studied their reactivity toward *cis*-$[M(C_6F_5)_2(thf)_2]$ (M = Pt, Pd). As shown in eq 2, treatment of *cis*-$[Pt(C{\equiv}CR)_2L_2]$ with 1 equiv of *cis*-$[M(C_6F_5)_2(thf)_2]$ (M = Pt, Pd) in CH_2Cl_2 at room temperature affords the homo- or heterobinuclear derivatives $[\{L_2Pt(\mu\text{-}\eta^1{:}\eta^2\text{-}C{\equiv}CR)_2\}M(C_6F_5)_2]$ (**5**−**12**) in good yield. These complexes, isolated as white microcrystalline solids, are moderately air-stable in the solid state but in solution they decompose in a few hours. The structural characterization of these dinuclear compounds is based on microanalysis, positive ion FAB mass spectrometry, and spectroscopic methods (IR (Table 1) and ^1H, ^{19}F, and ^{31}P NMR (Table 2)). In agreement with a dimeric formulation, the FAB(+) mass spectra show the expected peak corresponding to the molecular ion in most of the complexes (Table 1).

Table 3. Relevant ^{13}C NMR Spectral Data of Several Complexes[a]

	$Pt-C_\alpha{\equiv}$	$\equiv C_\beta-R$	$P-C_\alpha{\equiv}$	$\equiv C_\beta-R$
	$[Pt(C{\equiv}CR)_2(PPh_2C{\equiv}CR)_2]$			
1	101.3 [1150]	109.3 (Ph) [313.9]	81 (101.6)	107.9 (Ph)
2	84.7 [1145]	117 (Bu^t) [309]	81.8 (98.2)	107.2 (Ph)
3	102.3	108.8 (Ph) [∼310]	70.7 (105.5)	118.3 (Bu^t)
4	85.4 [1135]	116.4 (Bu^t) [307]	71.5 (101.7)	117.5 (Bu^t)
	$[\{PPh_2C{\equiv}CR)_2Pt(\mu\text{-}\eta^1{:}\eta^2\text{-}C{\equiv}CR)_2\}Pt(C_6F_5)_2]$			
5	90.5	103.8 (Ph)	78.7 (112)	109.3 (Ph)
7	83.2	113.9 (Bu^t)	79.5 (109)	108.6 (Ph)
9	91	103.2 (Ph)	68.7 (115)	120.0 (Bu^t)
11	84.1	113.3 (Bu^t)	69.4 (112)	119.2 (Bu^t)
	$[\{cis\text{-}Pt(\mu\text{-}\kappa(P){:}\eta^2\text{-}PPh_2C{\equiv}CPh)_2(\mu\text{-}\eta^1{:}\eta^2C{\equiv}CBu^t)_2\}\{Pt(C_6F_5)_2\}_2]$			
15A	87.7	124.6 (Bu^t)	78.3 (77.8)	109.5 (Ph)
	$[\{PPh_2C{\equiv}CBu^t)_2Pt(\mu_3\text{-}\eta^2\text{-}C{\equiv}CPh)_2\}\{Pt(C_6F_5)_2\}_2]$			
16B			67.5 (126.7)	121.4
	$[\{cis\text{-}Pt(\mu\text{-}\kappa(P){:}\eta^2\text{-}PPh_2C{\equiv}CBu^t)_2(\mu\text{-}\eta^1{:}\eta^2C{\equiv}CBu^t)_2\}\{Pt(C_6F_5)_2\}_2]$			
18A	87.18	*c* (Bu^t)	70.5 (97.1)	113.2 (Bu^t)

[a] R = $PPh_2C{\equiv}CPh$, $PPh_2C{\equiv}CBu^t$. [b] Numbers in brackets are $^1J_{C-Pt}$ or $^3J_{C-Pt}$; numbers in parentheses are $^1J_{C-P}$. [c] A badly resolved signal at 108.9 (m) can be tentatively assigned to this C_β carbon.

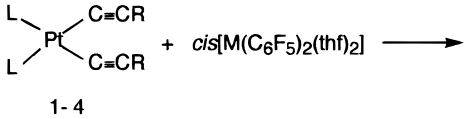

1-4

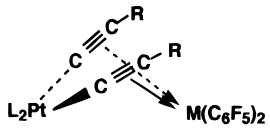

(2)

R	L	M
Ph	$PPh_2C{\equiv}CPh$	Pt **5**, Pd **6**
Ph	$PPh_2C{\equiv}CBu^t$	Pt **7**, Pd **8**
Bu^t	$PPh_2C{\equiv}CPh$	Pt **9**, Pd **10**
Bu^t	$PPh_2C{\equiv}CBu^t$	Pt **11**, Pd **12**

The presence of terminal phosphinoalkyne ligands is inferred from the IR spectra. Thus, all complexes show ν(C≡C) absorptions assignable to the phosphinoalkyne ligands which lies approximately in the same region as in the corresponding mononuclear derivatives. As in the precursors, complexes **5**−**8** (L = $PPh_2C{\equiv}CPh$) only exhibit one strong ν(C≡C) absorption (range 2179−2175 cm^{-1}), while in the $PPh_2C{\equiv}CBu^t$ complexes (**9**−**12**), two absorptions in the range 2212−2168 cm^{-1} are seen. One is assigned to ν(C≡C), and the other one is assigned to a Fermi resonance observed in substituted *tert*-butylalkynes.[10] Moreover, in concordance with the η^2-coordination of the alkynyl entities, some of the compounds (**6**−**8** and **12**) also show additional weak (C≡C)

(7) (a) Cross, R. J.; Gemmill, J. *J. Chem. Soc., Dalton Trans.* **1984**, 199. (b) Bradshaw, J. D.; Guo, L.; Tessier, C. A.; Youngs, W. J. *Organometallics* **1996**, *15*, 2582. (c) Pregosin, P. S.; Kunz, R. W. In *NMR Basic Principles and Progress*; Diehl, P., Fluck, E., Kosfeld, R., Eds.; Springer-Verlag: New York, 1979; Vol. 16, pp 43−45.

(8) (a) Sebald, A.; Wrackmeyer, B. *Z. Naturforsch.* **1983**, *38b*, 1156. (b) Sebald, A.; Wrackmeyer, B.; Beck W. *Z. Naturforsch.* **1983**, *38b*, 45. (c) Sebald, A.; Stader, C.; Wrackmeyer, B.; Bensh, W. *J. Organomet. Chem.* **1986**, *311*, 233.

(9) Berenguer, J. R.; Forniés, J.; Lalinde, E.; Martínez, F. *Organometallics* **1996**, *15*, 4537.

(10) Grindley, T. B.; Johnson, K. F.; Katritzky, A. R.; Keogh, H. J.; Thirkettle, C.; Topsom, R. D. *J. Chem. Soc., Perkin Trans. II* **1974**, 282.

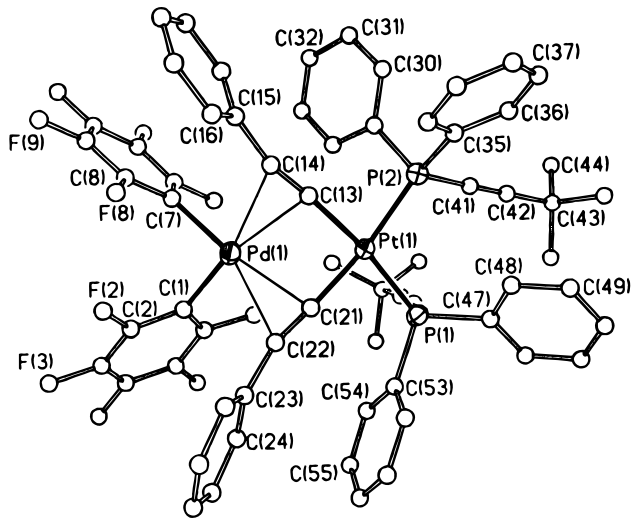

Figure 1. View of the molecular structure of [{($Bu^tC{\equiv}CPh_2P)_2Pt(\mu\text{-}\eta^1{:}\eta^2\text{-}C{\equiv}CPh)_2\}Pd(C_6F_5)_2$], **10**.

Table 4. Selected Bond Lengths (Å) and Angles (deg) for 10

Pt(1)−C(21)	1.972(4)	Pt(1)−C(13)	1.983(4)
Pt(1)−P(1)	2.2639(10)	Pt(1)−P(2)	2.2783(11)
Pt(1)−Pd(1)	3.1582(11)	Pd(1)−C(1)	1.986(4)
Pd(1)−C(7)	2.003(3)	Pd(1)−C(21)	2.283(3)
Pd(1)−C(13)	2.314(3)	Pd(1)−C(22)	2.433(4)
Pd(1)−C(14)	2.456(4)	P(1)−C(59)	1.729(4)
P(1)−C(47)	1.796(4)	P(1)−C(53)	1.803(4)
P(2)−C(41)	1.735(4)	P(2)−C(29)	1.801(4)
P(2)−C(35)	1.813(4)	C(13)−C(14)	1.205(5)
C(21)−C(22)	1.210(5)	C(41)−C(42)	1.189(5)
C(59)−C(60)	1.177(5)		
C(21)−Pt(1)−C(13)	81.87(14)	C(21)−Pt(1)−P(1)	91.21(10)
C(13)−Pt(1)−P(2)	89.76(11)	P(1)−Pt(1)−P(2)	97.16(4)
C(1)−Pd(1)−C(7)	83.87(14)	C(1)−Pd(1)−C(21)	99.93(14)
C(7)−Pd(1)−C(13)	104.58(13)	C(21)−Pd(1)−C(13)	68.59(13)
C(1)−Pd(1)−C(22)	80.77(13)	C(7)−Pd(1)−C(14)	83.05(13)
C(14)−C(13)−Pt(1)	175.8(3)	C(14)−C(13)−Pd(1)	82.0(2)
C(13)−C(14)−C(15)	166.2(4)	C(22)−C(21)−Pt(1)	175.7(3)
C(22)−C(21)−Pd(1)	82.1(2)	Pt(1)−C(21)−Pd(1)	95.57(14)
C(21)−C(22)−C(23)	164.5(4)	C(42)−C(41)−P(2)	175.3(4)
C(41)−C(42)−C(43)	177.6(5)	C(60)−C(59)−P(1)	165.7(4)
C(59)−C(60)−C(61)	176.3(4)		

absorptions at lower frequencies (range 2068−2040 cm^{-1}), which is in keeping with the presence of bridging alkynyl ligands. Unfortunately, this expected absorption assignable to the $Pt(\mu\text{-}C{\equiv}CR)_2M$ moiety is not observed in the rest of the complexes. So, in order to confirm the assignment made above, an X-ray diffraction study has been carried out on a single crystal of one of the complexes, **10**. A drawing of the structure is presented in Figure 1, and selected bond distances (Å) and angles (deg) are collected in Table 4. A relevant feature of this structure is the presence of a palladium atom coordinated to two mutually *cis*-σ C_6F_5 groups and stabilized by a chelating bis(alkynyl)platinum(II) fragment "*cis*-$[Pt(C{\equiv}CPh)_2(PPh_2C{\equiv}CBu^t)_2]$" through unusual η^2-alkynide interactions. In spite of the fact that the reactivity of alkynes toward palladium(II) complexes has been extensively explored,[11] only a few complexes

Scheme 2

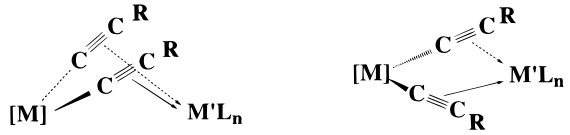

containing an η^2-palladium(II)−alkyne moiety have been reported.[6c,9,12] These types of complexes have been proposed as intermediates in the final formation of unusual molecules arising from insertion and/or polymerization processes at the Pd(II) center.[13] Due to the peculiar ability of bis(alkynyl)platinum substrates to stabilize unusual η^2-metal−alkyne interactions, we have previously isolated and reported the first two examples $[\{cis\text{-}Pt(C_6F_5)_2(\mu\text{-}\eta^1{:}\eta^2\text{-}C{\equiv}CSiMe_3)_2\}Pd(\eta^3\text{-}C_3H_5)]^-$ [6c] and $[\{cis\text{-}(PPh_3)_2Pt(\mu\text{-}\eta^1{:}\eta^2\text{-}C{\equiv}CBu^t)_2\}Pd(\eta^3\text{-}C_3H_5)]^+$ [9] containing structural information about an η^2-alkyne interaction to a cationic palladium center "$Pd(C_3H_5)^+$". Complex **10** represents a new example in which two C≡CPh ligands are η^2-coordinated to an electrophilic neutral palladium(II) center of the "$Pd(C_6F_5)_2$" building block.

The palladium center is located in a slightly distorted square-planar environment formed by two η^2-C≡C bonds (C(13)−C(14), C(21)−C(22)) and two σ-C_6F_5 ligands, the dihedral angle between the planes Pd−C(1)−C(7) and Pd(1)−M1−M2 (M1 and M2 are the midpoints of C(13)≡C(14) and C(21)≡C(22)) being only 6.6°. As found in the cation $[\{cis\text{-}(PPh_3)_2Pt(\mu\text{-}\eta^1{:}\eta^2\text{-}C{\equiv}CBu^t)_2\}Pd(\eta^3\text{-}C_3H_5)]^+$,[9] the η^2-palladium alkynido linkages in **10** are asymmetric with the Pd−C_α distances approximately 0.15 Å shorter than the corresponding Pd−C_β (Pd(1)−C(13), Pd(1)−C(21) 2.314(3), 2.283(3) Å versus Pd(1)−C(14), Pd(1)−C(22) 2.456(4), 2.433(4) Å, respectively). This asymmetry, although less pronounced than that found in the cation $[\{cis\text{-}(PPh_3)_2Pt(\mu\text{-}\eta^1{:}\eta^2\text{-}C{\equiv}CBu^t)_2\}Pd(\eta^3\text{-}C_3H_5)]^+$ [9] ($\Delta \sim 0.2$ Å), contrasts with the symmetrical η^2-linkages found in the anion $[\{cis\text{-}Pt(C_6F_5)_2(\mu\text{-}\eta^1{:}\eta^2\text{-}C{\equiv}CSiMe_3)_2\}Pd(\eta^3\text{-}C_3H_5)]^-$ [6c] and in the neutral dinuclear complex $[\{(dppe)Pt(\mu\text{-}\eta^1{:}\eta^2\text{-}C{\equiv}CR)_2\}Pt(C_6F_5)_2]$,[6a] in which both alkynyl ligands of the neutral 3-platinapenta-1,4-diyne neutral fragment are also η^2-coordinated to a similar $M(C_6F_5)_2$ building block. The angles formed by the C≡C vectors and the normal to the palladium coordination plane (Pd, C(1), C(7), M1, and M2) are 48.6(2)° for C(13,14) and 46.7(2)° for C(21,22). This structural feature clearly forces the Pd center to be located out of the 3-platina-1,4-diyne plane (Pt, C(13), C(14), C(21), C(22)) by 1.309(2) Å, resulting in a central bent dimetallacycle PtC_4Pd core (the dihedral angle formed by the Pd and Pt coordination planes is 58.46(6)°). A similar structural feature (type **I**, Scheme 2) has been found in other

(11) (a) Maitlis, P. M.; Espinet, P.; Rusell, M. J. H. In *Comprehensive Organometallic Chemistry*; Wilkinson, G., Stone, F. G. A., Abel, E. W., Eds.; Pergamon Press: Oxford, U.K., 1982; Vol. 6, Chapters 38.5 and 38.9. (b) Maitlis, P. M. *Acc. Chem. Res.* **1976**, *9*, 93. (c) Maitlis, P. M. *J. Organomet. Chem*. **1980**, *200*, 161. (d) Huggins, J. M.; Bergman, R. G. *J. Am. Chem. Soc.* **1981**, *103*, 3002. (e) Samsel, E. G.; Norton, J. R. *J. Am. Chem. Soc.* **1984**, *106*, 5505.

(12) (a) $[Pd_2Cl_4(Bu^tC{\equiv}CBu^t)_2]$: Hosokawa, T.; Moritani, I.; Nishioka, S. *Tetrahedron Lett*. **1969**, 3833. (b) *cis*-$[Pd(C_6F_5)_2(PhC{\equiv}CPh)_2]$: Usón, R.; Forniés, J.; Tomás, M.; Menjón, B.; Welch, A. J. *J. Organomet. Chem*. **1986**, *304*, C24. (c) Recently, several palladium(II) complexes containing η^1-metallacarbyne ligands (including X-ray and theoretical studies) have been reported: (i) Engel, P. F.; Pfeffer, M.; Dedieu, A. *Organometallics* **1995**, *14*, 3423. (ii) Engel, P. F.; Pfeffer, M.; Fisher, J.; Dediu, A. *J. Chem. Soc., Chem. Commun.* **1991**, 1275.

(13) (a) Ryabov, A. D.; van Eldik, R.; Le Borgne, G.; Pfeffer, M. *Organometallics* **1993**, *12*, 1386 and references therein. (b) Backvall, J.-E.; Nilson, Y. I. M.; Gatti, R. G. P. *Organometallics* **1995**, *14*, 4242 and references therein. (c) Zhn, G.; Lu, X. *Organometallics* **1995**, *14*, 4899.

dinuclear chelating $[M](\mu\text{-}C{\equiv}CR)_2M'L_n$ complexes containing $M'L_n$ building blocks with square-planar environments at M′.[6a−d] However, this structural conformation (type **I**, Scheme 2) contrasts with that typically found in other well-known heterometallic tweezer-like complexes in which the M′ center is well embedded by bis(alkynyl)titanocene fragments displaying almost planar TiC_4M' cores (type **II**, Scheme 2).[14] The factors responsible for the preferred *in* or *out*-η^2 alkyne−M bonding interaction in this type of adduct are still poorly understood. For instance, the only reported examples in which a bis(alkynyl)platinum fragment forms tweezer-like adducts correspond to $[\{(C_6F_5)_2Pt(C{\equiv}CSiMe_3)_2\}MX_2]^{2-}$ (MX_2 = $HgBr_2$[15] and $CoCl_2$[16]). In these anions, the preference of the chelated metal center for *in*-plane η^2-alkyne−M bonding interactions could be ascribed to their resulting tetrahedral environments with lower steric requirements. However, in the related trinuclear anion $[\{(Pt(C{\equiv}CBu^t)_2\}(CoCl_2)_2]^{2-}$, the η^2-alkyne cobalt bonding interactions take place *out* of the $Pt(C{\equiv}C)_2$ entities[16] and the bending of the central PtC_4Co cores is accompanied by a significant decrease in the Pt−Co distance (0.44 Å). It was suggested that the weak attraction between the basic platinum and acidic cobalt centers (3.007 Å) appears to drive the distortion of the PtC_4Co core from planarity and, hence, determines the final *out*-of-plane η^2-alkyne−cobalt interactions. In complex **10**, the Pt···Pd distance is also rather long (3.1582(11) Å), excluding any metal−metal interaction.

As a consequence of the η^2-coordination of the two arms of the 3-platina-1,4-diyne fragment *cis*-$[Pt(C{\equiv}CPh)_2(PPh_2C{\equiv}CBu^t)_2]$ to the palladium atom Pd(1), the following structural features arise: (i) slight bending of the Pt−$C_\alpha{\equiv}C_\beta$−C units from linearity (angles at C_α 175.8(3)°/175.7(3)° and at C_β 166.2(4)°/164.5(4)°) which is comparable to those found in related systems[6,9,14−16] and (ii) a slight decrease of the bite angle C(13)−Pt(1)−C(21) (81.87(14)°) with respect to the expected value of 90°. It should be noted that this decrease (∼9°) is slightly larger than those found in the tweezer-like derivatives $[\{Pt(C_6F_5)_2(C{\equiv}CSiMe_3)_2\}MX_2]$ (MX_2 = $HgBr_2$ 88.0(9)°,[15] $CoCl_2$ 86.5(9)° [16]).

Apart from the above considerations, all other distances and angles in the organometallic platinum fragment *cis*-$[Pt(C{\equiv}CPh)_2(PPh_2C{\equiv}CBu^t)_2]$ are within the expected ranges[17] (see Table 4). In particular, the C≡C bond lengths 1.189(5), 1.177(5) Å and angles 165.7(4)°, 177.6(5)° in the phosphinoalkyne ligands are those expected for noncoordinated phosphinoalkynes,[17] although the entity P(1)−C(59)−C(60) (165.7(4)°) is slightly more deviated from linearity, probably due to steric effects.

The relative orientation of the two $PPh_2C{\equiv}CPh$ ligands is of interest. The C(41)≡C(42) bond vector is oriented almost perpendicular to C(59)≡C(60) (71.9(4)°), but the linear alkynyl moieties do not cross one another. The triple bonds are rotated away from one another, and the separation between the two C_α carbon atoms is very large (3.355(5) Å). Carty *et al.* have established a relationship between the facility of intramolecular coupling of uncoordinated alkyne triple bonds in phosphinoalkynes and the proximity between the α-carbon atoms of the proximal alkyne units.[17b] Thus, the dichloro complex *cis*-$[PtCl_2(PPh_2C{\equiv}CPh)_2]$ with the linear alkynyl moieties "crossed" and with a $C_\alpha{-}C_\alpha$ separation of 3.110(10) Å undergoes alkyne coupling under relatively mild conditions. However, our compound with the triple bonds rotated shows no evidence of coupling below its decomposition temperature.

The ^1H, ^{19}F, and ^{31}P NMR data for dinuclear complexes **5**−**12** are consistent with the solid-state structure of complex **10**. Thus, ^1H NMR spectra of *tert*-butylacetylide-bridged complexes (**7**, **8**, **11**, and **12**) show, besides multiplets due to the phenyl protons, a singlet at 0.78 (**7**, **8**) or 0.76 (**11**, **12**) ppm due to the equivalent Bu^t groups, which remain as singlets even at −50 °C. In addition, complexes **11** and **12** show another singlet at 0.99 (**11**) or 1.00 (**12**) ppm attributed to the Bu^t groups on the terminal $PPh_2C{\equiv}CBu^t$ units, as in complexes **9** and **10** (δ 1.03 ppm). The equivalent phosphorus atoms of the terminal phosphinoalkyne ligands in these dinuclear derivatives appear in the ^{31}P NMR spectra at systematically lower frequencies (range from δ −8.53 to −13.06) with respect to the values observed in the precursors (δ −5.87 to −7.90). The magnitude of $^1J_{Pt-P}$ (2644−2692 Hz) is slightly larger than in the corresponding mononuclear homologues with terminal C≡CR groups (2311−2360 Hz), suggesting that the *trans* influence of a bridging alkynyl ligand is presumably smaller.

As is obvious from Figure 1, the two C_6F_5 groups in these dinuclear derivatives (**5**−**12**) are equivalent but the two halves of each C_6F_5 ring are inequivalent. Accordingly, room temperature ^{19}F NMR spectra of complexes with *tert*-butylacetylide bridging ligands (**7**, **8**, **11**, and **12**) display the expected five signals of equal intensity, thus indicating a rigid structure on the NMR time scale. In contrast, the NMR spectra of complexes **5**, **6**, **9**, and **10** with phenylacetylide bridging ligands show only three signals of relative intensity 2:1:2, evidencing that the two halves of each C_6F_5 ring appear equivalent at room temperature and indicating that these complexes are not rigid in solution. By lowering the temperature (−50 °C), five distinct fluorine resonances are clearly resolved for the diplatinum derivatives only (**5**, **9**). When the heterobinuclear derivatives $[L_2Pt(\mu\text{-}C{\equiv}CPh)Pd(C_6F_5)_2]$ **6** (L = $PPh_2C{\equiv}CPh$) and **10** (L = $PPh_2C{\equiv}CBu^t$) are cooled, their spectra remain unchanged indicating equivalence of the *endo* and *exo* *o*-F atoms (and *m*-F atoms as well) even at low temperature (−50 °C). This equivalence can be achieved by either of the two following processes: (i) free rotation of the C_6F_5 groups about the M−C linkages or (ii) fast exchange of the $M(C_6F_5)_2$ unit below and above the 3-platina-1,4-diyne fragments $L_2Pt(C{\equiv}CPh)_2$. Although the first possibility has been previously noted as severely sterically hindered in square-planar derivatives,[18] it has been proposed in several systems[19] and could be accessible *via* tricoordinate species through the cleavage

(14) (a) Janssen, M. D.; Köhler, K.; Herres, M.; Dedieu, A.; Smeets, W. J. J.; Spek, A. L.; Grove, D. M.; Lang, H.; van Koten, G. *J. Am. Chem. Soc.* **1996**, *118*, 4817 and references therein. (b) Janssen, M. D.; Herres, M.; Sepk, A. L.; Grove, D. M.; Lang, H.; Van Koten, G. *J. Chem. Soc., Chem. Commun.* **1995**, 925. (c) Lang, H.; Herres, M.; Imohof, W. *J. Organomet. Chem.* **1994**, *464*, 283. (d) Lang, H.; Blau, S.; Nuber, B.; Zsolnai, L. *Organometallics* **1995**, *14*, 3216 and references therein. (e) Lang, H.; Köhler, K.; Büchner, M. *Chem. Ber.* **1995**, *128*, 525.

(15) Berenguer, J. R.; Forniés, J.; Lalinde, E.; Martín, A.; Moreno, M. T. *J. Chem. Soc., Dalton Trans.* **1994**, 3343.

(16) Ara, I.; Berenguer, J. R.; Forniés, J.; Lalinde, E. *Inorg. Chim. Acta*, in press.

(17) (a) Carty, A. J.; Taylor, N. J.; Johnson, D. K. *J. Am. Chem. Soc.* **1979**, *101*, 5422. (b) Johnson, D. K.; Rukachaisirikul, T.; Sun, Y.; Taylor, N. J.; Canty, A. J.; Carty, A. J. *Inorg. Chem.* **1993**, *32*, 5544.

of one of the M−alkyne bonds.[20] The second possibility, previously suggested by us in the related complexes $[L_2Pt(\mu\text{-}C{\equiv}CR)_2Pt(C_6F_5)_2]$ (L = PPh_3, dppe, COD),[6a] implies a formal inversion of the central PtC_4M (M = Pd, Pt) cores. This inversion could take place *via* intermediate species with one or both alkynyl ligands symmetrically bridging the two metal centers.[21] The results indicate that this process is less favorable for the *tert*-butylalkynide-bridged complexes than for phenyl compounds because of the lower total energy required by the phenyl complexes to reach the transition state which is stabilized by the phenyl π electrons. Notwithstanding, in these derivatives, exchange mechanisms that entail $PPh_2C{\equiv}CR$ participation cannot be excluded either.

The very low stability of the mixed Pt−Pd derivatives (**6**, **8**, **10**, and **12**) in solution prevented their characterization by ^{13}C NMR spectroscopy. This was, however, possible for the diplatinum **5**, **7**, **9**, and **11** compounds (see Experimental Section and Table 3). The most noticeable observation is that upon η^2-coordination of the alkynyl ligands to the platinum atoms, the resonances of both C_α and C_β carbon atoms moves slightly upfield. A similar upfield shift of alkynyl carbon signals has been previously observed in the formation of dimeric $[X_2Pt(\mu\text{-}C{\equiv}CR)_2Pd(C_3H_5)]^-$ (X = C_6F_5, C≡CR)[9] complexes containing alkynyl bridging ligands. It should be noted that this result contrasts with previous observations, showing that η^2-complexation of terminal alkynyl ligands to a second metal center results in a downfield shift of these signals.[14d,22] On the other hand, although the alkyne carbon resonances of the phosphinoalkyne ligands are less affected in the formation of these dimeric complexes, the $P{-}C_\alpha{\equiv}$ carbon signals are also slightly shifted upfield while the $\equiv C_\beta{-}R$ signals move downfield. In addition, the values of the $^1J_{P-C_\alpha}$ coupling constants are slightly larger in these complexes (109−115 Hz) than those observed in the precursors **1**−**4** (98.2−105.5 Hz) (see Table 3). It should be noted that in complexes **7** and **11**, the signals due to the phenyl rings of the $PPh_2C{\equiv}CR$ ligands are observed to be magnetically inequivalent, probably because of the hindered rotation across the Pt−P bonds.

Trinuclear Derivatives. In order to force the coordination of the *P*-bonded phosphinoalkyne ligands, the reactions of the mononuclear complexes **1**−**4** with 2 equiv of *cis*-$[M(C_6F_5)_2(thf)_2]$ (M = Pt, Pd) were also explored. The results, summarized in Scheme 3, clearly indicate that the course of the reactions and the final products strongly depend on the alkynyl substituents, both in the alkynido and phosphinoalkyne ligands and in the metal centers.

The *tert*-butylacetylide complexes *cis*-$[Pt(C{\equiv}CBu^t)_2L_2]$ (L = $PPh_2C{\equiv}CPh$ (**2**), $PPh_2C{\equiv}CBu^t$ (**4**)) react with 2.2 equiv of *cis*-$[Pt(C_6F_5)_2(thf)_2]$ to give the desired trinuclear derivatives **15A** and **18A**, respectively, in moderate yield (see Experimental Section). In these complexes (type **A**), the mononuclear precursors (**2**, **4**) act as symmetrical bis(*cis*-η^2:$\kappa(P)$:η^2) chelating tetradentate ligands. Therefore, the complexed *cis*-$Pt(C_6F_5)_2$ units are linked to the central platinum atom through both a *tert*-butylalkynyl fragment (μ-η^2-C≡CBu^t) and a diphenylalkynylphosphine bridging ligand (μ-$\kappa(P)$:η^2), as established by an X-ray diffraction study on complex **15A** (vide infra). NMR (^{31}P and ^{19}F) monitoring of both reactions clearly indicates that the formation of complexes **15A** and **18A** takes place *via* the corresponding dinuclear derivatives **7** and **11**, respectively. Initially (within seconds), the formation of **15A**/**7** and **18A**/**11** mixtures in ratios of 80:20 and ∼10:90, respectively, were observed (see Scheme 3). The gradual disappearance of **7** and concomitant formation of **15A** is clean and takes place completely in ∼1 h. However, the evolution of the reaction system **4**/*cis*-$[Pt(C_6F_5)_2(thf)_2]$ is more complicated due to the much slower formation of **18A** and to its low stability in solution; it reverts to the dinuclear derivative. The greatest amount of **18A** in solution is reached after 3 h (**18A**/**11** ratio ≈ 83:11), and with longer reaction times, the concentration of **18A** decreases while that of **11** increases (a 55/45 ratio after 7 h). The formation of **15A** and **18A** through the corresponding dinuclear derivatives requires a reorganization of the bonded *cis*-$Pt(C_6F_5)_2$ unit and a significant reorientation of both phosphinoalkyne groups. It seems likely that this latter process should be somewhat more difficult with the bulkier $PPh_2C{\equiv}CBu^t$ groups, thus explaining the observed slower reaction rate for complex **18A**. Attempts to prepare the $PtPd_2$ analogues of **15A** and **18A** failed. When 2 equiv of *cis*-$[Pd(C_6F_5)_2(thf)_2]$ is reacted with the mononuclear *tert*-butylalkynido derivatives **2** and **4** in dichloromethane, very dark brown solutions are formed from which only the dinuclear complexes **8** and **12**, respectively, can be isolated. In the case of the reaction between **4** and *cis*-$[Pd(C_6F_5)_2(thf)_2]$, the NMR spectra in $CDCl_3$ of the reaction mixture reveals that the dinuclear complex **12** is the only phosphorus-containing platinum species present in solution. The ^{19}F NMR spectrum confirms the presence of excess *cis*-$Pd(C_6F_5)_2(thf)_2$ and shows the formation of considerable amounts of decafluorobiphenyl ($C_6F_5{-}C_6F_5$). If the $C_6F_5{-}C_6F_5$ formed comes from a possible trinuclear coordination complex, it has a lifetime that is too short to allow observation by NMR spectroscopy. NMR examination of the crude product of the reaction mixture between **2** and *cis*-$[Pd(C_6F_5)_2(thf)_2]$ reveals that, at low temperature (−50 °C), the dinuclear complex **8** is formed almost instantaneously and an excess of *cis*-$[Pd(C_6F_5)_2(thf)_2]$ is the only other solute present. When the temperature was increased to room temperature, considerable decomposition takes place (Pd, $C_6F_5{-}C_6F_5$) together with concomitant formation of other new unidentified platinum phosphine complexes (^{31}P NMR $\delta(P)$ 37.6 (d), 33.8 (m), 31.4 (d), 27.5 (d)). Unfortunately, the low relative amounts of these species and the very low stability of the reaction mixture at room temperature precluded their identification.

(18) (a) Albéniz, A. C.; Cuevas, J. C.; Espinet, P.; de Mendoza, J.; Prados, P. *J. Organomet. Chem.* **1991**, *410*, 257. (b) Abel, E. W.; Orrell, K. G.; Osborne, A. G.; Pain, H. M.; Sik, W.; Hursthouse, M. B.; Malik, K. M. A. *J. Chem. Soc., Dalton Trans.* **1994**, 3441.

(19) (a) Berenguer, J. R.; Forniés, J.; Lalinde, E.; Martínez, F.; Urriolabeitia, E.; Welch, A. *J. Chem. Soc., Dalton Trans.* **1994**, 1291. (b) Ara, I.; Berenguer, J. R.; Forniés, J.; Lalinde, E.; Tomás, M. *Organometallics* **1996**, *15*, 1014. (c) Falvello, L. R.; Forniés, J.; Navarro, R.; Rueda, A.; Urriolabeitia, E. P. *Organometallics* **1996**, *15*, 309.

(20) (a) Casares, J. A.; Coco, S.; Espinet, P.; Lin, Y.-S. *Organometallics* **1995**, *14*, 3058. (b) Minniti, D. *Inorg. Chem.* **1994**, *33*, 2631.

(21) Berenguer, J. R.; Falvello, L.; Forniés, J.; Lalinde, E.; Tomás, M. *Organometallics* **1993**, *12*, 6.

(22) (a) Erker, G.; Fromberg, W.; Benn, R.; Mynott, R.; Angermund, K.; Krüger, C. *Organometallics* **1989**, *8*, 911. (b) Falvello, L. R.; Fernández, S.; Forniés, J.; Lalinde, E.; Martínez, F.; Moreno, M. T. *Organometallics* **1997**, *16*, 1326.

Scheme 3

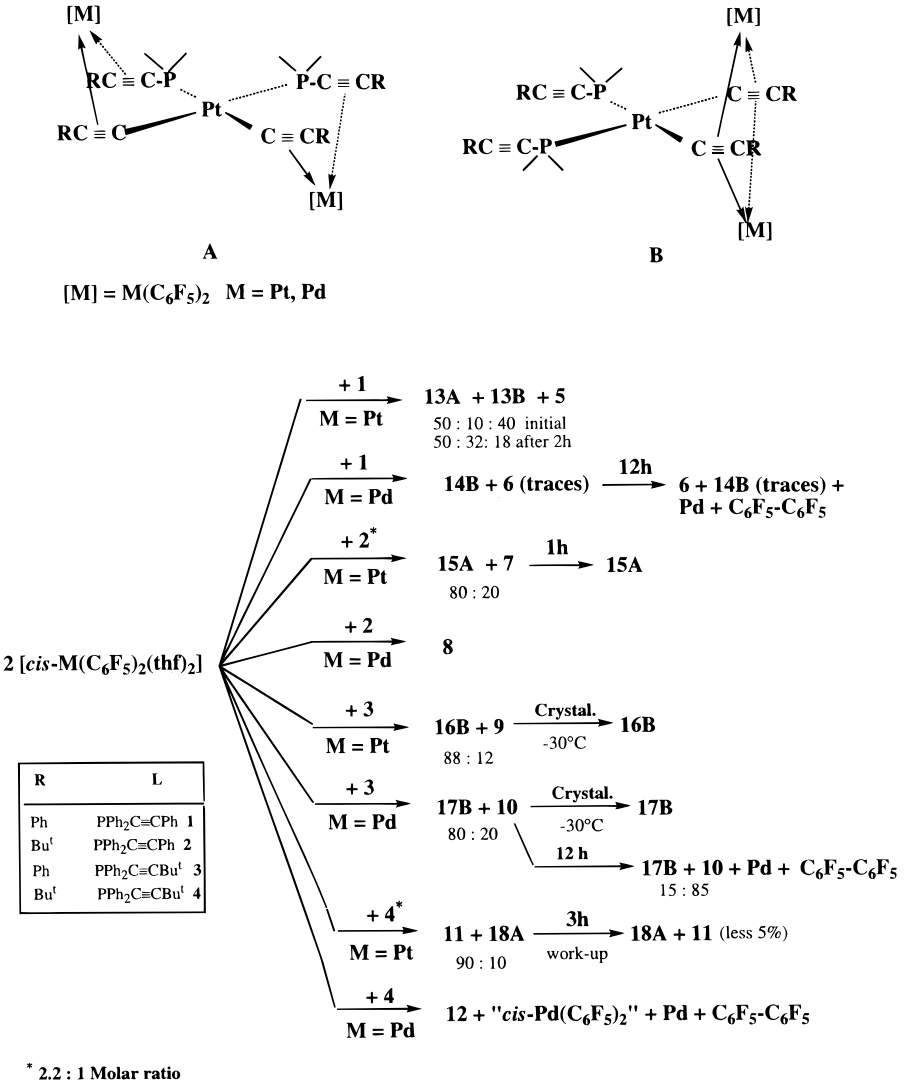

As shown in Scheme 3 (see Experimental Section), similar reactions of 2 equiv of *cis*-[Pd(C_6F_5)$_2$(thf)$_2$] with the *cis*-bis(phenylacetylide)bis((diphenylphosphino)-alkyne) platinum complexes **1** and **3** in CH_2Cl_2 instantaneously yield a new type of triangular $PtPd_2$ complexes (**14B** and **17B**) together with small amounts of the corresponding dinuclear derivatives **6** (traces, less than 5%) and **10** (~20%), respectively, as proven by NMR spectroscopy (^{31}P and ^{19}F). Crystallization of the crude mixture at low temperature (CH_2Cl_2/hexane interface) gave a pure sample of **17B**. Both derivatives are stable at low temperature (~−30 °C) as solids but rapidly decompose in $CDCl_3$ at room temperature (~12 h) to the corresponding dinuclear derivatives, depositing Pd metal and giving, probably through a reductive elimination process, a considerable amount of C_6F_5−C_6F_5. An analogous reaction between complex **3** (L = $PPh_2C{\equiv}CBu^t$) and 2 equiv of *cis*-[Pt(C_6F_5)$_2$(thf)$_2$] also gives a similar mixture of **9** and the new triangular Pt_3 complex **16B** instantaneously, which is an isomer of **15A**, in an approximate 15:85 mixture from which pure **16B** can be isolated as a white microcrystalline solid in high yield (45%) after work-up. The structure of complex **16B**, which is stable both as a solid and in solution ($CDCl_3$) has been determined by X-ray crystallography, confirming that in this case the $PPh_2C{\equiv}CBu^t$ groups act as terminal ligands and both phenylethynylalkyl fragments behave as six-electron donors (μ_3-η^2, σ,π,π). Finally, the reaction between **1** (L = $PPh_2C{\equiv}CPh$) and 2 equiv of *cis*-[Pt(C_6F_5)$_2$(thf)$_2$] is less selective, giving both isomers **13A** and **13B** in a 50:32 ratio and ~80% conversion (dinuclear complex **5**, ~18%, is also present) after a reaction time of 2 h. Interestingly, NMR (^{31}P and ^{19}F) examination of this reaction shows (Scheme 3) an initial **13A**:**13B**:**5** mixture in a 50:10:40 ratio. After 2 h, the signals assigned to complex **5** clearly have diminished while the proportion of **13B** has increased significantly. No detectible change was observed after 8 h, with the final ratio being ~50:32:18 as mentioned above. Several attempts to separate at least the dominant component (**13A**) were unsuccessful; therefore, both derivatives have been characterized spectroscopically only on the basis of their NMR properties (mainly ^{31}P), which are similar to these of the rest of the complexes.

Both types of trinuclear complexes (**A** and **B**) display very characteristic spectroscopic data consistent with the corresponding formulation shown in Scheme 3 and in agreement with the structures of **15A** and **16B** presented in Figures 2 and 3, respectively. Thus, in the IR spectra of complexes **15A** and **18A**, there are only characteristic absorptions (see Table 1) in the expected range for complexed carbon−carbon triple bonds,[6,9,14,19a,22] thus confirming that all acetylene fragments are in-

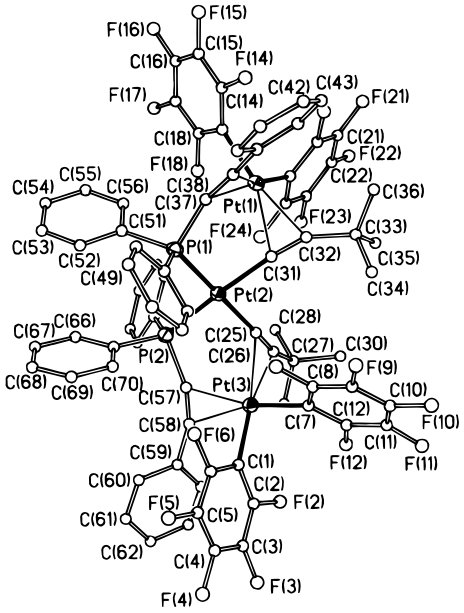

Figure 2. Drawing of the molecular structure of [{Pt(μ-$\kappa(P)$:η^2-$PPh_2C{\equiv}CPh)_2$(μ-η^1:η^2-$C{\equiv}CBu^t)_2$}{$Pt(C_6F_5)_2$}$_2$], **15A**.

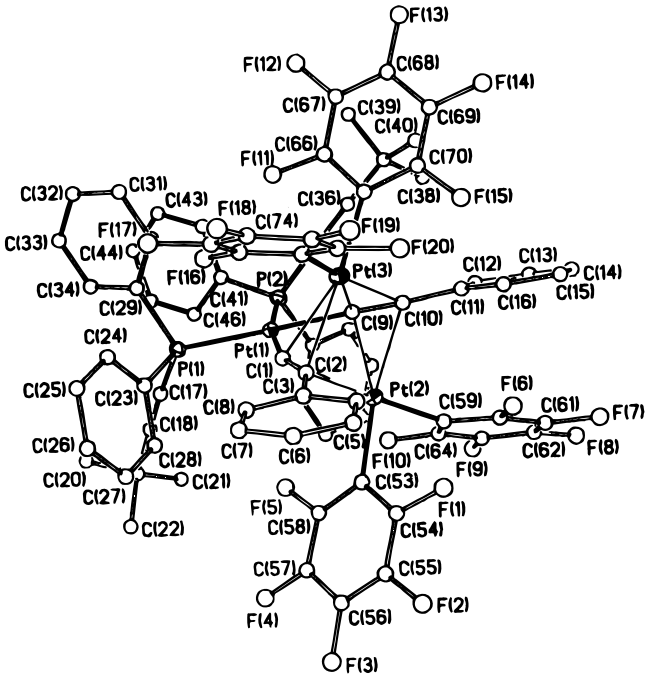

Figure 3. Molecular structure of [{$(PPh_2C{\equiv}CBu^t)_2Pt$($\mu_3$-$\eta^2$-$C{\equiv}CPh)_2$}{$Pt(C_6F_5)_2$}$_2$], **16B**.

volved in side-on coordination. In contrast, the IR spectra of complexes **14B**, **17B** ($PtPd_2$), and **16B** ($PtPt_2$) show two strong ν(C≡C) absorptions in the range 2151−2210 cm^{-1}, indicating the presence of a terminal phosphinoalkyne ligand. All three complexes exhibit additional weak ν(C≡C) bands at lower frequencies (1951 cm^{-1} (**14B**), 1883, 1870 (sh) (**16B**), and 1951 cm^{-1} (**17B**)), evidencing the presence of bridging alkynyl ligands. It should be noted that in accord with the behavior of alkynyl groups as six-electron donors, this shift to lower frequencies (cf ν(C≡C) at 2124 and 2117 cm^{-1} in **1** and **3**, respectively) is significantly more pronounced than that observed for the dinuclear complexes in which ν(C≡C) can be observed (range 2068−2040 cm^{-1}; 1951 cm^{-1} in **14B** *vs* 2068 cm^{-1} in **6**).

Characteristic of the presence of (diphenylphosphino)-alkyne bridging ligands in complexes of type **A** is a considerable downfield shift of the ^{31}P (δP) resonance ($\delta(P)$ −0.92 (**15A**), −1.96 (**18A**), and 0.67 (**13A**)) with respect to that observed in the mononuclear precursors (−6.13 (**2**), −7.76 (**4**), −5.87 (**1**)) or in the corresponding dinuclear derivatives in which the $PPh_2C{\equiv}CR$ molecules act only as *P*-donor ligands (−10.56 (**7**), −13.06 (**11**), −10.4 (**5**)). This spectroscopic fact can be attributed to the characteristic formation of (both) dimetallacycles in which the $PPh_2C{\equiv}CR$ ligands are involved as bridging ligands. However, the platinum−phosphorus coupling constants (2488 (**15A**), 2501 (**18A**), 2524 Hz (**13A**)) are less affected, being slightly larger than those observed for the starting precursors (2311 (**2**), 2335 (**4**), 2343 Hz (**1**)) but slightly smaller than those seen for the dinuclear complexes (2674 (**7**), 2689 (**11**), 2679 Hz (**5**)).

In contrast, the equivalent phosphorus atoms of the terminal phosphinoalkyne moieties in complexes of type **B** appear in the ^{31}P NMR spectra as singlets clearly shifted to lower frequencies ($\delta(P)$ −19.5 (**13B**), −14.10 (**14B**), −20.55 (**16B**), −14.80 (**17B**)) with respect to the values observed in the precursors (−5.87 (**1**), −7.90 (**3**)) and in the corresponding dinuclear derivatives (range −8.53 (**6**) to −12.79 (**9**)). Moreover, all $^1J_{Pt-P}$ coupling constants are extraordinarily large (range from 2891 Hz for **14B** to 3008 Hz for **16B**) compared to the range observed for either mononuclear and dinuclear complexes (see Table 2). This points to a weaker σ-interaction between Pt(1) and the C_α carbon atoms of the alkynyl ligands due to their additional interaction with the remaining two platinum centers (σ-Pt(1), π-Pt(2), π-Pt(3)) which seem to be compensated by stronger interactions with the *P*-bonded phosphinoalkyne ligands. Unfortunately, the ^{13}C NMR spectrum of complex **16B** is not informative (see Experimental Section and Table 3) since the $Pt-C_\alpha{\equiv}$ carbon resonances could not be located in spite of prolonged accumulation. The spectra of **14B** and **17B** could not be obtained due to their very low stability in solution.

The ^{19}F NMR spectra of both types of complexes (**A** and **B**) are temperature dependent (see Table 2). For instance, at low temperature (−50 °C), complex **15A** displays two different sets of five fluorine signals (two F_o, F_p, and two F_m), in keeping with the presence of two inequivalent rigid C_6F_5 groups in which both halves of each ring are inequivalent (AFMRX system). When the temperature is increased, the two *ortho* and two *meta* fluorine resonances of one of the sets clearly broaden and, finally, collapse to only two broad signals at room temperature (∼288 K) giving a $\Delta G^{\ddagger}$ (T_c) value of approximately 53 KJ/mol for the process that renders the *o*-F resonances equivalent.[23] The remaining five signals due to one of the C_6F_5 rings appear sharp at this temperature (room temperature). The spectra can be tentatively explained by assuming that the presence of different ligands *trans* to the C_6F_5 rings (alkynyl and phosphinoalkyne) induces different energy barriers on their rotation around the $Pt-C_{ipso}(C_6F_5)$ bonds. Thus, at low temperature the rotation seems to be stopped for both rings, but at higher temperatures this process is faster for one of them, averaging the two F_o (and the two F_m) resonances. A similar behavior has been found previously in other complexes containing the *cis*-Pt-

(23) Günther, H. *NMR Spectroscopy*; Wiley: New York, 1980; p 241.

Table 5. Selected Bond Lengths (Å) and Angles (deg) for 15A·0.5C_6H_{12}·0.45C_6H_5

Pt(1)−C(19)	2.009(8)	Pt(3)−C(7)	2.020(8)
Pt(1)−C(38)	2.257(8)	Pt(3)−C(58)	2.294(8)
Pt(2)−C(25)	2.012(8)	P(1)−C(37)	1.769(8)
Pt(2)−P(1)	2.282(2)	C(27)−C(29)	1.506(13)
Pt(3)−C(57)	2.179(8)	Pt(1)−C(37)	2.219(7)
Pt(3)−C(26)	2.322(8)	Pt(1)−C(31)	2.315(8)
C(26)−C(27)	1.489(11)	Pt(2)−P(2)	2.271(2)
C(37)−C(38)	1.233(11)	Pt(3)−C(1)	2.034(8)
Pt(1)−C(13)	2.046(8)	Pt(3)−C(25)	2.307(8)
Pt(1)−C(32)	2.299(8)	C(25)−C(26)	1.220(11)
Pt(2)−C(31)	2.015(8)	C(31)−C(32)	1.211(11)
C(19)−Pt(1)−C(13)	85.2(3)	C(13)−Pt(1)−C(37)	93.2(3)
C(13)−Pt(1)−C(38)	93.6(3)	C(19)−Pt(1)−C(32)	86.7(3)
C(38)−Pt(1)−C(32)	91.9(3)	C(19)−Pt(1)−C(31)	99.1(3)
C(37)−Pt(1)−C(31)	77.9(3)	C(25)−Pt(2)−C(31)	90.2(3)
C(25)−Pt(2)−P(2)	81.5(2)	C(31)−Pt(2)−P(2)	169.2(2)
C(31)−Pt(2)−P(1)	89.3(2)	P(2)−Pt(2)−P(1)	99.38(7)
C(7)−Pt(3)−C(1)	86.0(3)	C(1)−Pt(3)−C(57)	100.9(3)
C(1)−Pt(3)−C(58)	80.6(3)	C(7)−Pt(3)−C(25)	92.9(3)
C(57)−Pt(3)−C(25)	76.0(3)	C(7)−Pt(3)−C(26)	92.5(3)
C(57)−Pt(3)−C(26)	85.5(3)	C(26)−C(25)−Pt(2)	166.5(7)
C(25)−C(26)−C(27)	162.1(8)	C(32)−C(31)−Pt(2)	172.7(7)
C(31)−C(32)−C(33)	153.9(8)	C(38)−C(37)−P(1)	154.6(7)
C(37)−C(38)−C(39)	160.5(8)	C(58)−C(57)−P(2)	160.9(7)
C(57)−C(58)−C(59)	160.6(8)	Pt(1)−Pt(2)−Pt(3)	35.1(1)

$(C_6F_5)_2CO$ fragment, which also has different ligands *trans* to the pentafluorophenyl groups.[19a,b] The behavior of **18A** is not clear (see Table 2 for data), as the two sharp F_p triplets observed at room temperature, in accord with the two expected types of C_6F_5 rings, also broaden when the temperature is lowered. At −50 °C, two sets of two overlapping triplets are seen, suggesting that at low temperature the complex is rigid and all C_6F_5 groups are inequivalent.

Similarly, in agreement with the behavior of the phenylacetylide precursors **1** and **3** as chelating tetradentate bridging ligands binding through the alkynyl groups to both *cis*-$M(C_6F_5)_2$ units, the ^{19}F NMR spectra of **14B**, **17B**, and **16B** at room temperature exhibit a single set of three signals (2:1:2; $2F_o$, F_p, $2F_m$) evidencing that all C_6F_5 groups are equivalent. The resonances assignable to F_o and F_m are very broad, also suggesting the existence of a dynamic process. On lowering the temperature, splitting occurs and the expected pattern corresponding to an AFMRX system is observed for all complexes at −50 °C. Using the coalescence temperatures given in Table 2 and the chemical shift difference on F_o at 223 K, $\Delta G^{\ddagger}$ (T_c) values of 52.1 (**14B**), 47.6 (**16B**), and 51.9 (**17B**) KJ/mol are obtained.[23] The spectrum of complex **17B** remains unaffected in the presence of an excess of *cis*-$[Pd(C_6F_5)_2(thf)_2]$, suggesting an intramolecular exchange process.

Crystal Structures of [{Pt(μ-κ(*P*):η²-$PPh_2C{\equiv}CPh$)$_2$(μ-η¹:η²-$C{\equiv}CBu^t$)$_2$}{$Pt(C_6F_5)_2$}$_2$] (15A·0.5C_6H_{14}·0.45C_6H_6) and [{($PPh_2C{\equiv}CBu^t$)$_2$Pt(μ$_3$-η²-$C{\equiv}CPh$)$_2$}{$Pt(C_6F_5)_2$}$_2$] (16B). The structure of the trinuclear complex **15A** is presented in Figure 2 together with the atom-labeling scheme used. Selected bond distances and angles are collected in Table 5. As shown, the most remarkable feature is that both terminal *cis*-$Pt(C_6F_5)_2$ moieties are linked to the central platinum atom through both an alkynyl unit (μ-η²) and a phosphinoalkyne ligand (μ-κ(*P*):η²). To the best of our knowledge, this is the first organometallic species possessing such a structure.

The platinum atoms have basically square-planar geometries, but their coordination environments are different. The central Pt(2) atom is bound to the C_α atoms of the two $C{\equiv}CBu^t$ groups, which are mutually *cis*, and to the two P atoms of the two $PPh_2C{\equiv}CPh$ ligands. The alkyne entities ($C{\equiv}CBu^t$ and $PPh_2C{\equiv}CPh$) are each η²-coordinated to both terminal Pt(1) and Pt(3) atoms, which complete their coordination environment with the C_{ipso} atoms of the two C_6F_5 groups, also mutually *cis*. This structural disposition indicates that again the reaction between complex **2** and 2 equiv of *cis*-$[Pt(C_6F_5)_2(thf)_2]$ proceeds with retention of the original configuration about the platinum centers. It should be noted, however, that the formation of complex **15A** through the dinuclear derivative **7** as an intermediate (complex **15A** is also formed starting from **7** and 1 equiv of *cis*-$[Pt(C_6F_5)_2(thf)_2]$) requires at least a minor movement of the initial *cis*-$Pt(C_6F_5)_2$ unit bonded.

Both terminal platinum atoms Pt(1) and Pt(3) are held in the complex by almost symmetrical π-bonding interactions to the carbon−carbon triple bonds (the most asymmetric interaction is found with the P−C(57)≡C(58)−Ph acetylenic fragment Pt(3)−C(57) 2.179(8) Å; Pt(3)−C(58) 2.294(8) Å) with typical Pt(1,3)−$C_{\alpha,\beta}$ distances (2.179(8)−2.322(8) Å).[6] The C−C alkyne distances at the acetylenic carbons of the $PPh_2C{\equiv}CPh$ ligands (1.233(11), 1226(11) Å) are similar to the corresponding ones involving the $C{\equiv}CBu^t$ alkynyl groups (1.220(1), 1.211(11) Å) but, as expected, longer than those observed for complexes **10** (average 1.183(5) Å) and **16B** (average 1.184(13) Å) which have terminal $PPh_2C{\equiv}CBu^t$ ligands. These distances are within the typical range of an alkyne bonded to transition metals that do not strongly back-bond.[4,6,15,16,19a] The acetylenic skeletons are slightly distorted from linearity, with the bend at the C_α carbon atoms more pronounced on the P−C_α−C_β−Ph entities (P−C_α−C_β 154.6(7)°, 160.9(7)° *vs* Pt−C_α−C_β 166.5(7)°, 172.7(7)°). The angles at the C_β carbon atoms are 162.1(8)° and 153.9(8)° on the Pt−C_α−C_β−C(Bu^t) entities and 160.5(8)°, 160.6(8)° at the P−C_α−C_β−C(Ph) fragments. The difference in the values of the platinum coupling constants between the dinuclear and trinuclear derivatives (**A** and **B**) is not reflected in the platinum−phosphorus bond lengths, which are identical within experimental error (mean values 2.277(2) (**15A**), 2.271(10) (**10**), 2.276(2) Å (**16B**)). As expected, the compound is not planar. The dihedral angles between the best least-squares coordination planes of each platinum center are Pt(1) plane−Pt(2) plane = 82.9°, Pt(2) plane−Pt(3) plane = 80.35°, and Pt(1) plane−Pt(3) plane = 68.13°. The observed Pt(2)−Pt(1,3) separations (3.560(1) and 3.597(1) Å) exclude the possibility of metal−metal bonding.

A perspective drawing of the structure of complex **16B** is depicted in Figure 3 together with the atom-numbering scheme. A summary of the important bond distances and angles is given in Table 6. As shown, in this complex the precursor fragment **3** acts a chelating tetradentate ligand bound through the alkynyl groups, giving a triangular Pt_3 core with intermetallic angles close to 60°. The Pt_3 plane is bicapped by two triply bridging phenylacetylide groups which are bonded in a μ$_3$-η² (σ,2π) fashion. Thus, both alkynyl ligands remain σ-bonded to Pt(1) (Pt(1)−C(1,9) 2.013(9), 2.001(9) Å) and are π-bonded to Pt(2) and Pt(3) with platinum−carbon distances in the range 2.266(9)−2.408(9) Å. It is interesting to note that these distances and the C_α

Table 6. Selected Bond Lengths (Å) and Angles (deg) for 16B

Pt(1)−C(9)	2.001(9)	Pt(3)−C(71)	2.009(9)
Pt(1)−P(2)	2.281(2)	Pt(3)−C(10)	2.337(9)
Pt(2)−C(59)	2.009(9)	P(1)−C(17)	1.742(9)
Pt(2)−C(1)	2.330(8)	C(9)−C(10)	1.270(12)
Pt(2)−Pt(3)	3.0982(5)	Pt(1)−P(1)	2.271(2)
Pt(3)−C(9)	2.311(8)	Pt(1)−Pt(2)	3.2219(5)
Pt(3)−C(2)	2.375(9)	Pt(2)−C(2)	2.266(9)
C(1)−C(2)	1.263(11)	Pt(2)−C(10)	2.408(9)
Pt(1)−C(1)	2.013(9)	Pt(3)−C(65)	2.028(9)
Pt(1)−Pt(3)	3.1973(5)	Pt(3)−C(1)	2.360(9)
Pt(2)−C(53)	2.011(9)	P(2)−C(35)	1.733(10)
Pt(2)−C(9)	2.337(8)	C(17)−C(18)	1.180(12)
C(9)−Pt(1)−C(1)	76.2(3)	C(1)−Pt(1)−P(1)	96.3(3)
C(9)−Pt(1)−P(2)	91.2(2)	P(1)−Pt(1)−P(2)	96.36(9)
Pt(3)−Pt(1)−Pt(2)	57.715(12)	C(59)−Pt(2)−C(53)	88.9(4)
C(53)−Pt(2)−C(2)	87.4(3)	C(53)−Pt(2)−C(1)	100.6(3)
C(59)−Pt(2)−C(9)	101.7(3)	C(1)−Pt(2)−C(9)	64.1(3)
C(59)−Pt(2)−C(10)	84.7(3)	C(2)−Pt(2)−C(10)	97.8(3)
Pt(3)−Pt(2)−Pt(1)	60.744(12)	C(71)−Pt(3)−C(65)	87.4(4)
C(65)−Pt(3)−C(9)	104.0(3)	C(71)−Pt(3)−C(10)	164.0(4)
C(65)−Pt(3)−C(10)	91.3(3)	C(9)−Pt(3)−C(10)	31.7(3)
C(71)−Pt(3)−C(1)	100.2(3)	C(65)−Pt(3)−C(1)	154.6(3)
C(9)−Pt(3)−C(1)	64.0(3)	C(71)−Pt(3)−C(2)	83.7(3)
C(10)−Pt(3)−C(2)	96.7(3)	Pt(2)−Pt(3)−Pt(1)	61.541(11)
C(2)−C(1)−Pt(1)	163.4(8)	C(1)−C(2)−C(3)	152.5(9)
C(1)−C(2)−Pt(2)	76.9(6)	C(1)−C(2)−Pt(3)	73.9(6)
Pt(2)−C(2)−Pt(3)	83.7(3)	C(10)−C(9)−Pt(1)	168.9(7)
C(10)−C(9)−Pt(3)	75.3(5)	C(9)−C(10)−C(11)	150.9(9)
C(9)−C(10)−Pt(3)	73.0(6)	C(9)−C(10)−Pt(2)	71.4(5)
Pt(3)−C(10)−Pt(2)	81.5(3)	C(18)−C(17)−P(1)	170.2(9)
C(17)−C(18)−C(19)	178.6(10)	C(35)−C(36)−C(37)	176.6(11)
C(36)−C(35)−P(2)	175.6(10)		

(168.9(7)°, 163.4(8)°) and C_β (150.9(9)°, 152.5(9)°) bending of the alkynyl ligands are comparable to the parameters found in [(dppe)Pt(μ-η^2-C≡CPh)$_2$Pt(C$_6$F$_5$)$_2$] (Pt(2)−C 2.269(13)−2.345(12) Å; angles at C_α 167.2°/159.2° and at C_β 164.6°/156.2°) in which the 3-platina-1,4-alkyne fragment chelates only one Pt(C$_6$F$_5$)$_2$ fragment.[6a] However, the carbon−carbon triple bond distances are, as expected, slightly longer (1.270(12), 1.263(11) Å in **16B** *vs* 1.229(17), 1.234(16) Å in the dinuclear derivative),[6a] and the bite angle C(1)−Pt(1)−C(9) of 76.2(3)° is only slightly smaller than that found in [(dppe)Pt(μ-η^2-C≡CPh)Pt(C$_6$F$_5$)$_2$] (79.3(4)°).

The platinum−platinum distances (Pt(1)−Pt(2,3) 3.2219(5), 3.1973(5) Å and Pt(2)−Pt(3) 3.0982(5) Å) are consistent with nonbonding interactions. As expected, the geometry around the platinum atoms is approximately square planar. An interesting structural feature is that, probably due to the presence of two Pt(C$_6$F$_5$)$_2$ units above and below the Pt(1) coordination plane, the chelating platinadiyne fragment [Pt(1)C(1)C(9)C(2)C(10)] is nearly planar (max deviation 0.020 Å for C(9)) with the phenyl substituents of the alkynyl ligands also lying in the same plane. The dihedral angles between these phenyl groups and the above platinadiyne plane are 38.0° and 36.5°, respectively.

The reasons for the final formation of these triangular molecules only with the phenylacetylide **1** and **3** precursors are difficult to discern, but the steric effects of the bulky *tert*-butylacetylide ligands cannot be discarded. Although several systems with two bridging alkynyl ligands have been reported so far [Os$_3$(CO)$_7$(μ-η^2C≡CPr^i)$_2$(μ-PPh$_2$)$_2$],[24a] [Os$_3$(μ-η^1-C$_2$R)(μ_3,η^2-C$_2$R)(CO)$_9$],[24b,c] [Ru$_3$(μ-η^1-C$_2$Bu^t)(μ-η^2-C$_2$Bu^t)(PPh$_2$)$_2$(CO)$_5$(PPh$_2$Bu^t)],[25] [Cu$_3$(μ_3-η^1-C≡CPh)$_2$(μ-dppm)$_3$](BF$_4$),[26] and [PtAg$_2$(C$_6$F$_5$)$_2$(μ-η^2,C≡CR)(μ_3-η^1-C≡CR)(PPh$_3$)$_2$],[27] to our knowledge the triangular Pt$_3$ core bicapped by two (μ-η^2-C≡CPh) ligands observed for **16B** is unprecedented.

Conclusion

The coordination ability of *cis*-bis(alkynyl)bis((diphenylphosphino)alkyne)platinum(II) complexes toward *cis*-[M(C$_6$F$_5$)$_2$(thf)$_2$] (M = Pt, Pd) has been studied. From this study, it is clear that the alkynyl (C≡CR) is the preferred bridging ligand. Thus, exclusive formation of double alkynyl bridging systems takes place in the formation of all 1:1 adducts (**5**−**12**). In addition, complexation *via* phenylethynyl fragments seems to predominate in the formation of trinuclear derivatives, as deduced from the following results: (i) complexation of the second *cis*-Pd(C$_6$F$_5$)$_2$ unit is only straightforward with the phenylethynyl substrates *cis*-[Pt(C≡CPh)$_2$L$_2$] (**1** and **3**) and takes place *via* C≡CPh groups which act as μ_3-η^2 bridging ligands; and (ii) while *cis*-[Pt(C≡CPh)$_2$(PPh$_2$C≡CBu^t)$_2$] (**3**) binds both *cis*-Pt(C$_6$F$_5$)$_2$ units through a double alkynyl bridging system (μ_3-η^2-C≡CPh)$_2$, **16B**), *cis*-[Pt(C≡CBu^t)$_2$(PPh$_2$C≡CPh)$_2$] (**2**) forms the isomeric symmetrical adduct [{Pt(μ-κ(*P*):η^2-PPh$_2$C≡CPh)$_2$(μ-η^1:η^2-C≡CBu^t)$_2$}{Pt(C$_6$F$_5$)$_2$}$_2$], **15A**, containing PPh$_2$C≡CPh bridging ligands. These results establish the order of bonding capability as follows: alkynyl > *P*-bonded phosphinoalkyne and C≡CPh units > C≡CBu^t units. Finally, the formation of complexes **15A** and **18A** clearly shows that the preference for η^2-alkyne−metal interactions is higher in platinum than in palladium substrates.

Experimental Section

General Methods. All reactions were carried out under N$_2$ using dried solvents purified by known procedures and distilled prior to use. IR spectra were recorded on a Perkin-Elmer 883 spectrometer from Nujol mulls between polyethylene sheets. NMR spectra were recorded on a Varian Unity 300 and a Bruker ARX 300 spectrometer. Chemical shifts are reported in ppm relative to external standards (SiMe$_4$, CFCl$_3$, and 85% H$_3$PO$_4$). Elemental analyses were carried out with a Perkin-Elmer 240-B microanalyzer and the mass spectra (FAB$^+$) on a VG Autospec spectrometer. [PPh$_2$C≡CPh],[28] [PPh$_2$C≡CBu^t],[28] [Pt(C≡CPh)$_2$COD],[29] [Pt(C≡CBu^t)$_2$COD],[6a] and *cis*-[Pt(C$_6$F$_5$)$_2$(thf)$_2$][30] were prepared by published procedures.

Synthesis of *cis*-[Pt(C≡CR)$_2$L$_2$] (L = L^1 = PPh$_2$C≡CPh, R = Ph (1), Bu^t (2); L = L^2 = PPh$_2$C≡CBu^t, R = Ph (3), Bu^t (4)). A typical preparation (complex **1**) was as follows: To a suspension of [Pt(C≡CPh)$_2$COD] (0.200 g, 0.396 mmol) in CH$_2$Cl$_2$ (10 cm^3) was added PPh$_2$C≡CPh (0.226 g, 0.791 mmol), immediately giving an orange solution. After the mixture was stirred for 10 min, the resulting solution was

(24) (a) Cherkas, A. A.; Taylor, N. J.; Carty, A. J. *J. Chem. Soc., Chem. Commun.* **1990**, 385. (b) Deeming, A. J.; Felix, M. S. B.; Bartes, P. A.; Hursthouse, M. B. *J. Chem. Soc., Chem. Commun.* **1987**, 461. (c) Deeming, A. J.; Felix, M. S. B.; Nuel, D. *Inorg. Chim. Acta* **1993**, *213*, 3.

(25) Carty, A. J.; Taylor, N. J.; Smith, W. F. *J. Chem. Soc., Chem. Commun.* **1979**, 750.

(26) (a) Díez, J.; Gamasa, M. P.; Gimeno, J.; Aguirre, A.; García-Granda, S. *Organometallics* **1991**, *10*, 380. (b) Díez, J.; Gamasa, M. P.; Gimeno, J.; Lastra, E.; Aguirre, A.; García-Granda, S. *Organometallics* **1993**, *12*, 2213.

(27) Ara, I.; Forniés, J.; Lalinde, E.; Moreno, M. T.; Tomás, M. *J. Chem. Soc., Dalton Trans.* **1994**, 2735; **1995**, 2397.

(28) Carty, A. J.; Hota, N. K.; Ng, T. W.; Patel, H. A.; O'Connor, T. J. *Can. J. Chem.* **1971**, *49*, 2706.

(29) Cross, R. J.; Davidson, M. F. *J. Chem. Soc., Dalton Trans.* **1986**, 1987.

(30) Usón, R.; Forniés, J.; Tomás, M.; Menjón, B. *Organometallics* **1985**, *4*, 1912.

evaporated to dryness. Then, the addition of cold diethyl ether (5 cm^3) gave **1** as a white solid.

Complexes **2**, **3**, and **4** were prepared similarly as white solids by using the appropriate starting materials. For complexes **3** and **4**, the resulting reaction mixtures were evaporated to dryness and the residue was treated with ^{i}PrOH giving the required products.

***cis*-[Pt(C≡CPh)$_2$(PPh$_2$C≡CPh)$_2$] (1) ^{13}C NMR (CDCl$_3$, 16 °C):** 133.4 (t, J_{CP} = 6.3 Hz, C$_o$, PPh$_2$), 131.8 (s, C$_o$, P−C≡CPh), 131.3 (s, $^4J_{Pt-C}$ = 8.8 Hz, C$_o$, C≡CPh), 130.6 (AXX′ five line pattern, $^1J_{CP}$ + $^3J_{CP}$ = 66.4 Hz, C$_i$, PPh$_2$), 130.2 (s, C$_p$, PPh$_2$), 129.5 (s, C$_p$, Ph), 127.9 (t, J_{CP} = 5.9 Hz, C$_m$, PPh$_2$), 127.8 (s, C$_m$, Ph), 126.8 (s, C$_m$, Ph), 124.9 (s, Ph), 120.6 (s, Ph), 109.3 (AXX′ five line pattern, $^3J_{CP_{trans}}$ + $^3J_{CP_{cis}}$ = 36.5 Hz, $^2J_{Pt-C_\beta}$ = 313.8 Hz, C$_\beta$, −C$_\alpha$≡C$_\beta$Ph), 107.9 (AXX′, $^2J_{CP}$ + $^4J_{CP}$ = 15.1 Hz, C$_\beta$, P−C$_\alpha$≡C$_\beta$Ph), 101.3 (dd, $^2J_{CP_{trans}}$ = 156.5 Hz, $^2J_{CP_{cis}}$ = 21.2 Hz, $^1J_{Pt-C_\alpha}$ = 1150 Hz, C$_\alpha$, −C$_\alpha$≡C$_\beta$Ph), 81.0 (dd, $^1J_{CP}$ = 101.6 Hz, $^3J_{CP}$ = 1.2 Hz, $^2J_{Pt-C}$ ≈ 17 Hz, C$_\alpha$, P−C$_\alpha$≡C$_\beta$Ph).

***cis*-[Pt(C≡CBu^t)$_2$(PPh$_2$C≡CPh)$_2$] (2) ^{13}C NMR (CDCl$_3$, 16 °C):** 133.6 (t, J_{CP} = 6.2 Hz, $^3J_{Pt-C}$ = 28.8, C$_o$, PPh$_2$), 131.7 (s, C$_p$, PPh$_2$), 131.4 (AXX′ five line pattern, $^1J_{CP}$ + $^3J_{CP}$ = 65 Hz, C$_i$, PPh$_2$), 129.8 (s, C$_o$, Ph), 129.2 (s, C$_p$, Ph), 127.7 (s, C$_m$, Ph), 120.9 (m, C$_i$, Ph), 117.0 (AXX′ five line pattern, $^3J_{CP_{trans}}$ + $^3J_{CP_{cis}}$ = 35.9 Hz, $^2J_{Pt-C}$ = 309 Hz, C$_\beta$, −C$_\alpha$≡C$_\beta$Bu^t), 107.2 (m, C$_\beta$, P−C$_\alpha$≡C$_\beta$Ph), 84.7 (dd, $^2J_{CP_{trans}}$ = 158 Hz, $^2J_{CP_{cis}}$ = 21.4 Hz, $^1J_{Pt-C_\alpha}$ = 1145 Hz, C$_\alpha$, −C$_\alpha$≡C$_\beta$Bu^t), 81.8 (dd, $^1J_{CP}$ = 98.2 Hz, $^3J_{CP}$ = 1.4 Hz, $^2J_{Pt-C}$ = 14 Hz, C$_\alpha$, P−C$_\alpha$≡C$_\beta$Ph), 31.45 (s, $^4J_{Pt-C}$ = 7.9 Hz, −C(*C*H$_3$)$_3$), 28.6 (s, $^3J_{Pt-C}$ = 21.4 Hz, −CMe$_3$).

***cis*-[Pt(C≡CPh)$_2$(PPh$_2$C≡CBu^t)$_2$] (3) ^{13}C NMR (CDCl$_3$, 16 °C):** 133.4 (t, J_{CP} = 6.2 Hz, Ph, C$_o$, PPh$_2$), 131.97 (AXX′ five line pattern, $^1J_{CP}$ + $^3J_{CP}$ = 66 Hz, C$_i$, PPh$_2$), 131.3 (s, Ph), 130.0 (s, C$_p$, PPh$_2$), 127.7 (t, J_{CP} = 6 Hz, C$_m$, PPh$_2$), 126.8 (s, Ph), 124.7 (s, Ph), 118.3 (t, J_{CP} = 7 Hz, C$_\beta$, −PC$_\alpha$≡C$_\beta$Bu^t), 108.8 (AXX′, $^3J_{C-P_{trans}}$ + $^3J_{C-P_{cis}}$ = 36 Hz, $^2J_{Pt-C}$ ≈ 310 Hz, C$_\beta$, −C$_\alpha$≡C$_\beta$-Ph), 102.3 (dd, $^2J_{C-P_{trans}}$ = 136 Hz, $^2J_{C-P_{cis}}$ = 21 Hz, Pt satellites are not observed, C$_\alpha$, −C$_\alpha$≡C$_\beta$Ph), 70.7 (d, J_{CP} = 105.5 Hz, C$_\alpha$, P−C$_\alpha$≡C$_\beta$Bu^t), 29.6 (s, −C(*C*H$_3$)$_3$), 28.1 (s, −*C*(Me$_3$)).

***cis*-[Pt(C≡CBu^t)$_2$(PPh$_2$C≡CBu^t)$_2$] (4) ^{13}C NMR (CDCl$_3$, 16 °C):** 133.6 (t, J_{CP} = 6.2 Hz, $^3J_{Pt-C}$ = 28.4, C$_o$, PPh$_2$), 132.8 (five line pattern AXX′, $^1J_{CP}$ + $^3J_{CP}$ = 65 Hz, C$_i$, PPh$_2$), 129.5 (s, C$_p$, PPh$_2$), 127.3 (t, J_{CP} = 5.8 Hz, C$_m$, PPh$_2$), 117.5 (t, J_{CP} = 6.5 Hz, C$_\beta$, −PC$_\alpha$≡C$_\beta$Bu^t), 116.4 (AXX′, $^3J_{C-P_{trans}}$ + $^3J_{C-P_{cis}}$ = 35.7 Hz, $^2J_{Pt-C_\beta}$ = 307 Hz, C$_\beta$, −C$_\alpha$≡C$_\beta$Bu^t), 85.4 (dd, $^2J_{C-P_{trans}}$ = 158.7 Hz, $^2J_{C-P_{cis}}$ = 21.2 Hz, $^1J_{Pt-C_\alpha}$ = 1135 Hz, C$_\alpha$, −C$_\alpha$≡C$_\beta$-Bu^t), 71.45 (d, $^1J_{CP}$ = 101.7 Hz, $^2J_{Pt-C}$ = 17.9 Hz, C$_\alpha$, −PC$_\alpha$≡C$_\beta$-Bu^t), 31.4 (s, −C(*C*H$_3$)$_3$, C$_\alpha$≡C$_\beta$Bu^t), 29.6 (s, −C(*C*H$_3$)$_3$, −PC$_\alpha$≡C$_\beta$-Bu^t), 28.5 (s, $^3J_{Pt-C}$ = 21.7 Hz, −*C*(Me$_3$), C$_\alpha$≡C$_\beta$Bu^t), 28.0 (s, −*C*(Me$_3$), −PC$_\alpha$≡C$_\beta$Bu^t).

Synthesis of [{L$_2$Pt(μ-η^1:η^2-C≡CR)$_2$}M(C$_6$F$_5$)$_2$] (L = L^1 = PPh$_2$C≡CPh, R = Ph, M = Pt (5), Pd (6); R = Bu^t, M = Pt (7), Pd (8); L = L^2 = PPh$_2$C≡CBu^t; R = Ph, M = Pt (9), Pd (10); R = Bu^t, M = Pt (11), Pd (12)). Synthesis of 5. To a solution of *cis*-[Pt(C≡CPh)$_2$(PPh$_2$C≡CPh)$_2$] (0.140 g, 0.144 mmol) in CH_2Cl_2 (20 cm^3) was added *cis*-[Pt(C$_6$F$_5$)$_2$(thf)$_2$] (0.097 g, 0.144 mmol), and the mixture was stirred at room temperature for 15 min. The resulting solution was concentrated to small volume (2 cm^3). Addition of *n*-hexane (3 cm^3) and standing at −30 °C gave **5** as a white crystalline product. Complexes **6**−**12** were prepared similarly using the appropriate starting materials.

[{(PhC≡CPh$_2$P)$_2$Pt(μ-η^1:η^2-C≡CPh)$_2$}Pt(C$_6$F$_5$)$_2$] (5) ^{13}C NMR (CDCl$_3$, 16 °C): 147.8, 144.8, 137.7, 134.5 (br, C$_6$F$_5$), 132.9 (t, J_{CP} = 6.6 Hz, C$_o$, PPh$_2$), 131.96 (s, Ph), 131.9 (s, Ph), 130.98 (s, Ph), 130.2 (AXX′ five line pattern, $^1J_{CP}$ + $^3J_{CP}$ = 69 Hz, C$_i$, PPh$_2$), 130.1 (s, C$_p$, Ph), 128.4 (t, J_{CP} = 6.1 Hz, C$_m$, PPh$_2$), 127.9 (s, C$_m$, Ph), 127.8 (s, C$_p$, Ph), 126.9 (s, C$_m$, Ph), 124.2 (s, C$_i$, Ph), 119.8 (s, C$_i$, Ph), 109.3 (AXX′, $^2J_{CP}$ + $^4J_{CP}$ = 17.3 Hz, C$_\beta$, P−C≡CPh), 103.8 (AXX′, five line pattern $^3J_{C-P_{trans}}$ + $^3J_{C-P_{cis}}$ = 30.5 Hz, C$_\beta$, −C$_\alpha$≡C$_\beta$Ph), 90.5 (dd, $^2J_{C-P_{trans}}$ = 145.5 Hz, $^2J_{C-P_{cis}}$ = 19.8 Hz, C$_\alpha$, −C$_\alpha$≡C$_\beta$Ph), 78.7 (d, $^1J_{CP}$ = 112 Hz, C$_\alpha$, −PC$_\alpha$≡C$_\beta$Ph).

[{(PhC≡CPh$_2$P)$_2$Pt(μ-η^1:η^2-C≡CBu^t)$_2$}Pt(C$_6$F$_5$)$_2$] (7) ^{13}C NMR (CDCl$_3$, 16 °C): 148.1 (m), 145.1 (m), 137.8 (m), 134.6 (m) (br, C$_6$F$_5$), 133.0 (m, overlapping of two triplets, C$_o$, PPh$_2$), 131.8 (s, C$_o$, Ph), 131.2 (AXX′, $^1J_{CP}$ + $^3J_{CP}$ = 45.7 Hz, C$_i$, PPh$_2$), ∼130.3 (C$_i$, PPh$_2$), 130.8 (s, C$_p$, PPh$_2$), 130.6 (s, C$_p$, PPh$_2$), 129.8 (s, C$_p$, Ph), 128.1 (m, overlapping of two triplets, C$_m$, PPh$_2$), 127.8 (s, C$_m$, Ph), 120.1 (s, C$_i$, Ph), 113.9 (m, C$_\beta$, C$_\alpha$≡C$_\beta$Bu^t, Pt satellites are not observed), 108.6 (m, C$_\beta$, P−C$_\alpha$≡C$_\beta$Ph), ∼83.2 (C$_\alpha$, −C$_\alpha$≡C$_\beta$Bu^t), 79.5 (d, J_{CP} = 109 Hz, C$_\alpha$, −PC$_\alpha$≡C$_\beta$Ph), 30.7 (s, −*C*(CH$_3$)$_3$), 30.1 (s, *C*Me$_3$).

[{(Bu^{t}C≡CPh$_2$P)$_2$Pt(μ-η^1:η^2-C≡CPh)$_2$}Pt(C$_6$F$_5$)$_2$] (9) ^{13}C NMR (CDCl$_3$, 16 °C): 147.8 (m), 144.9 (m), 137.6 (m), 134.4 (m, br, C$_6$F$_5$), 132.9 (t, J_{CP} = 6.6 Hz, C$_o$, PPh$_2$), 131.9 (s, Ph), 131.6 (AXX′ five line pattern, $^1J_{CP}$ + $^3J_{CP}$ = 69 Hz, C$_i$, PPh$_2$), 130.8 (s, C$_p$, PPh$_2$), 128.2 (t, J_{CP} = 6 Hz, C$_m$, PPh$_2$), 127.7 (s, C$_p$, Ph), 126.9 (s, C$_m$, Ph), 124.3 (s, C$_i$, Ph), 120.0 (m, C$_\beta$, −PC$_\alpha$≡C$_\beta$Bu^t), 103.2 (m, $^3J_{C-P_{trans}}$ + $^3J_{C-P_{cis}}$ = 30.6 Hz, C$_\beta$, −C$_\alpha$≡C$_\beta$Ph), 91.3 (dm, $^2J_{C-P_{trans}}$ ≈ 145 Hz, C$_\alpha$, −C$_\alpha$≡C$_\beta$Ph), 68.7 (d, $^1J_{CP}$ = 115 Hz, C$_\alpha$, −PC$_\alpha$≡C$_\beta$Bu^t), 29.5 (s, −*C*(CH$_3$)$_3$), 28.3 (s, *C*Me$_3$).

[{(Bu^{t}C≡CPh$_2$P)$_2$Pt(μ-η^1:η^2-C≡CBu^t)$_2$}Pt(C$_6$F$_5$)$_2$] (11) ^{13}C NMR (CDCl$_3$, 16 °C): 133.1 (C$_o$), 133.02 (C$_o$) (overlapping of two triplets PPh$_2$), 132.20 (C$_i$), 132.17 (C$_i$) (overlapping of two AXX′ fine line patterns), 130.5 (s, C$_p$, PPh$_2$), 127.97 (C$_m$), 127.85 (C$_m$) (overlapping of two triplets PPh$_2$), 119.2 (t, J_{CP} = 7.6 Hz, C$_\beta$, PC$_\alpha$≡C$_\beta$Bu^t), 113.3 (AXX′, $^3J_{C-P_{trans}}$ + $^3J_{C-P_{cis}}$ = 29.4 Hz, Pt satellites are not observed, C$_\beta$, −C$_\alpha$≡C$_\beta$Bu^t), 84.1 (dd, $^2J_{C-P_{trans}}$ = 145.9 Hz, $^2J_{C-P_{cis}}$ = 20.5 Hz, C$_\alpha$, C$_\alpha$≡C$_\beta$Bu^t), 69.4 (d, J_{CP} = 112 Hz, C$_\alpha$, −PC$_\alpha$≡C$_\beta$Bu^t), 30.7 (s, −*C*H$_3$), 30.08 (s, *C*Me$_3$), 29.5 (s, −*C*H$_3$), 29.2 (s, *C*Me$_3$).

Reaction of *cis*-[Pt(C≡CPh)$_2$L$^1_2$] (1) with *cis*-[Pt(C$_6$F$_5$)$_2$-(thf)$_2$] (Molar Ratio of 1:2). A mixture of *cis*-[Pt(C$_6$F$_5$)$_2$(thf)$_2$] (0.015 g, 0.022 mmol) and *cis*-[Pt(C≡CPh)$_2$(PPh$_2$C≡CPh)$_2$] (0.0108 g, 0.011 mmol) was dissolved in 0.6 cm^3 of $CDCl_3$, and the reaction was immediately monitored by NMR spectroscopy. Integration of the NMR signals shows an approximate 50:10:40 proportion of **13A**, **13B**, and **5** (Scheme 3). After 2 h, the intensity of the signal due to the dinuclear derivative **5** decreases while the signal attributed to **13** increases with the final proportion being **13A**:**13B**:**5** 50:32:18. An identical ratio was observed after 8 h.

All attempts to separate **13A** or **13B** from this reaction mixture were unsuccessful; thus, the complexes **13A** and **13B** were only characterized by spectroscopy: ^{1}H NMR ($CDCl_3$, ppm) δ 8.00−6.8 (m, **13A** + **13B**); ^{19}F NMR ($CDCl_3$, ppm) −116.5 (br), −117.2 (s, br) (F$_o$, **13A** + **13B**), −160.97 (t), −161.1 (t), −161.5 (t) (3F$_p$: 2 inequivalent F$_p$ from **13A** and 1 F$_p$ from **13B**), −164.1 (m), −164.6 (m) (F$_m$, **13A** + **13B**); ^{31}P{^{1}H} NMR ($CDCl_3$, ppm) 0.67 (s, $^1J_{Pt-P}$ = 2524 Hz, **13A**), −19.5 (s, $^1J_{Pt-P}$ = 2996 Hz, **13B**). The signal due to complex **5** (−10.8, $^1J_{Pt-P}$ = 2677 Hz) is also present.

Synthesis of [{L$^1_2$Pt(μ$_3$-η^{2}C≡CPh)$_2$}{Pd(C$_6$F$_5$)$_2$}$_2$], 14B. *cis*-[Pd(C$_6$F$_5$)$_2$(thf)$_2$] (0.100 g, 0.171 mmol) was added to a stirred solution of *cis*-[Pt(C≡CPh)$_2$(PPh$_2$C≡CPh)$_2$] (**1**; 0.083 g, 0.086 mmol) in CH_2Cl_2 (5 cm^3). The resulting solution was immediately evaporated to dryness, and the residue was treated with *n*-hexane (5 cm^3) to give a white powder (70% yield). The ^{31}P NMR spectrum of this solid shows it to be complex **14B** with a purity >95%. Only traces (less 5%) of complex **6** were also observed. On standing at room temperature (∼12 h), considerable decomposition to Pd metal takes place and the only species detected thereafter by ^{31}P{^{1}H} and ^{19}F spectroscopy were the dinuclear complex **6** and decafluorobiphenyl (C$_6$F$_5$−C$_6$F$_5$). Identical results were obtained starting from **6** and 1 equiv of *cis*-[Pd(C$_6$F$_5$)$_2$(thf)$_2$].

Synthesis of [{Pt(μ-κ(*P*):η^2-PPh$_2$C≡CPh)$_2$(μ-η^1:η^2-C≡CBu^t)$_2$}{Pt(C$_6$F$_5$)$_2$}$_2$], 15A. *cis*-[Pt(C$_6$F$_5$)$_2$(thf)$_2$] (0.152 g, 0.229 mmol) was added to a solution of [Pt(C≡CBu^t)$_2$-(PPh$_2$C≡CPh)$_2$] (**2**; 0.100 g, 0.107 mmol) in CH_2Cl_2 (10 cm^3), and the mixture was stirred for 1 h at room temperature. The resulting yellow solution was evaporated to dryness, and the residue was treated with a mixture of diethyl ether/hexane

Table 7. Crystal Data and Structure Refinement Parameters for Complexes 10·Me_2CO, 15A·0.5C_6H_{14}·0.45C_6H_6, and 16B[a]

complex	**10**·Me_2CO	**15A**·0.5C_6H_{14}·0.45C_6H_6	**16B**
empirical formula	$C_{64}H_{48}F_{10}P_2PdPt$·$Me_2CO$	$C_{76}H_{48}F_{20}P_2Pt_3$·0.5$C_6H_{12}$·0.45$C_6H_6$	$C_{76}H_{48}F_{20}P_2Pt_3$
fw	1428.53	2065.65	1988.35
unit cell dimens			
a (Å)	9.863(4)	14.0631(10)	14.8963(12)
b (Å)	15.314(5)	17.6645(12)	23.5869(11)
c (Å)	19.840(6)	17.9951(15)	19.8044(11)
α (deg)	88.46(2)	76.082(12)	90
β (deg)	86.71(1)	72.341(10)	100.596(8)
γ (deg)	82.54(2)	86.577(10)	90
volume (Å^3), *Z*	2966(2), 2	4134.2(6), 2	6839.8(7), 4
wavelength (Å)	0.710 73	0.710 73	0.710 73
temperature (K)	200	150	150
radiation	graphite-monochromated Mo Kα	graphite-monochromated Mo Kα	graphite-monochromated Mo Kα
cryst syst	triclinic	triclinic	monoclinic
space group	$P\bar{1}$	$P\bar{1}$	$P2_1/c$
cryst dimens (mm)	0.74 × 0.46 × 0.32	0.30 × 0.20 × 0.20	0.50 × 0.25 × 0.25
abs coeff (mm^{-1})	2.787	5.197	6.267
transmission factors	0.991, 0.630	0.438, 0.350	0.984, 0.625
abs corr	*ψ* scans	*ψ* scans	*ψ* scans
diffractometer	Siemens STOE/AED2	Enraf-Nonius CAD4	Enraf-Nonius CAD4
2*θ* range for data collection (deg)	2.1−24.0 (+*h*, ±*k*, ±*l*)	2.0−25.0 (+*h*, ±*k*, ±*l*)	2.0−25.0 (+*h*, +*k*, ±*l*)
no. of reflns collected	11 110	15 107	12 463
no. of indep reflns	9268 (*R*(int) = 0.0238)	14 465 (*R*(int) = 0.0298)	11 971 (*R*(int) = 0.0366)
refinement method	full-matrix least-squares on F^2	full-matrix least-squares on F^2	full-matrix least-squares on F^2
goodness-of-fit on F^2	1.043	1.002	1.048
final *R* indices ($I > 2\sigma(I)$)	R1 = 0.0239, wR2 = 0.0539	R1 = 0.0415, wR2 = 0.1077	R1 = 0.0432, wR2 = 0.0652
R indices (all data)	R1 = 0.0306, wR2 = 0.0586	R1 = 0.0633, wR2 = 0.1178	R1 = 0.0945, wR2 = 0.0789

[a] $R1 = \sum(|F_o| - |F_c|)/\sum|F_o|$; $wR2 = [\sum w(F_o^2 - F_c^2)^2/\sum w(F_c^2)^2]^{1/2}$. Goodness-of-fit = $[\sum w(F_o^2 - F_c^2)^2/(n_{obs} - n_{param})]^{1/2}$. $w = [\sigma^2(F_o) + (g_1P)^2 + g_2P]^{-1}$; $P = [\max(F_o^2; 0) + 2F_c^2]/3$.

(3/2). Cooling at −30 °C for 12 h gives complex **15A** as a pale yellow microcrystalline solid (0.18 g).

^{13}C NMR ($CDCl_3$, −50 °C): ∼146, 144, 138.1, 135.3 (br, C_6F_5), 134.5−128.5 (Ph), 124.6 (m, C_β, $-C_\alpha{\equiv}C_\beta Bu^t$), 119.4 (s, Ph), 109.5 (m, C_β, $-PC_\alpha{\equiv}C_\beta Ph$), 87.7 (dd, $^2J_{C-P_{trans}}$ = 151.8 Hz, $^2J_{C-P_{cis}}$ = 15.5 Hz, C_α, $-C_\alpha{\equiv}C_\beta Bu^t$), 78.3 (d, $^1J_{CP}$ = 77.76 Hz, C_α, $P-C_\alpha{\equiv}C_\beta Ph$), 30.7 (s, $-C(CH_3)_3$), 31.7, 22.7, 14.4 (s, hexane).

Reaction of *cis*-[Pt(C≡CBu^t)$_2$L$^1_2$] (2) with *cis*-[Pd(C_6F_5)$_2$(thf)$_2$] (Molar Ratio of 1:2). *cis*-[Pd(C_6F_5)$_2$(thf)$_2$] (0.025 g, 0.043 mmol) was added to a solution of *cis*-[Pt(C≡CBu^t)$_2$($PPh_2C{\equiv}CPh$)$_2$] (0.020 g, 0.0215 mmol) in $CDCl_3$ (0.6 cm^3), and a ^{31}P NMR spectrum was taken immediately. The initial $^{31}P\{^1H\}$ NMR spectrum of this mixture at low temperature (−50 °C) revealed the presence of complex **8** (−8.9 ppm) as the main component together with the excess of *cis*-[Pd(C_6F_5)$_2$(thf)$_2$]. When the temperature was increased to room temperature, considerable decomposition had taken place (Pd metal) and, in addition to complex **8**, small signals at ∼37.6 (d), 33.8 (m), 31.4 (d), and 27.5 (d) ppm were also observed. The ^{19}F NMR indicated the presence of a considerable amount of $C_6F_5-C_6F_5$.[31]

Synthesis of [{L$^2_2$Pt(μ_3-η^2C≡CPh)$_2$}{Pt(C_6F_5)$_2$}$_2$], 16B. To a solution of *cis*-[Pt(C≡CPh)$_2$($PPh_2C{\equiv}CBu^t$)$_2$] (**3**; 0.100 g, 0.1075 mmol) in CH_2Cl_2 (10 cm^3) was added 0.145 g (0.215 mmol) of *cis*-[Pt(C_6F_5)$_2$(thf)$_2$]. After 1 h of stirring, the brown solution was evaporated to dryness and the residue was treated with ^{i}PrOH (3 cm^3) to give a crude solid, which was washed with *n*-hexane. The ^{31}P NMR spectra of this solid indicates that complex **16B** is contaminated (∼12%) with the dinuclear derivative **9**. Complex **16B** is obtained as a white microcrystalline solid by slow crystallization of the crude material in a CH_2Cl_2/hexane (1:5) mixture at low temperature (−30 °C).

^{13}C{^{1}H} NMR ($CDCl_3$, −50 °C): 147.4, 144.3, 138.8 (br, C_6F_5), 133.8−126.8 (Ph), 121.37 (m, C_β, $P-C_\alpha{\equiv}C_\beta Bu^t$), 119.7 (s, Ph), 67.5 (d, $^1J_{C-P}$ = 126.7, C_α, $P-C_\alpha{\equiv}C_\beta Bu^t$), 29.3 (s, $C(CH_3)_3$), 28.5 (s, CMe_3).

Synthesis of [{L$^2_2$Pt(μ_3-η^2C≡CPh)$_2$}{Pd(C_6F_5)$_2$}$_2$], 17B. *cis*-[Pt(C≡CPh)$_2$($PPh_2C{\equiv}CBu^t$)$_2$] (**3**; 0.0608 g, 0.0654 mmol) and 0.0764 g (0.1307 mmol) of *cis*-[Pd(C_6F_5)$_2$(thf)$_2$] were mixed in CH_2Cl_2 (5 cm^3), and the resulting solution was immediately evaporated to dryness. The residue was extracted with hexane (2 × 5 cm^3), giving a beige solid (**17B**:**10** ≈ 90:10 by ^{31}P NMR). Recrystallization of this solid (CH_2Cl_2/hexane interface at −30 °C) yielded **17B** as a colorless powder.

When the reaction was monitored by $^{31}P\{^1H\}$ NMR spectroscopy at 20 °C, we identified a mixture of **17B** and **10** (ratio 80:20). After longer periods, considerable decomposition of **17B** is observed. Thus, in 12 h the intensity of the signal due to **17B** decreases, giving a **17B**/**10** ratio of ∼15:85. In addition, the ^{19}F NMR spectrum reveals the presence of considerable amounts of decafluorobiphenyl.

Synthesis of [{Pt(μ-κ(*P*):η^2-$PPh_2C{\equiv}CBu^t$)$_2$(μ-η^1:η^2-C≡CBu^t)$_2$}{Pt(C_6F_5)$_2$}$_2$], 18A. Complex **4** (0.072 g, 0.081 mmol) in CH_2Cl_2 (10 cm^3) was treated with 0.120 g (0.178mmol) of *cis*-[Pt(C_6F_5)$_2$(thf)$_2$] for 3 h. The resulting solution was evaporated to dryness, and the crude solid (**18A** + **11** (83:17) by ^{31}P NMR) was treated with *n*-hexane, giving **18A** as a nearly pure solid (less than 5% of **11** is detected by ^{31}P NMR). Yield: 57%. If the initial mixture is stirred for longer periods, complex **18A** decomposes increasing the amount of **11**. Thus, in 7 h, the intensity of the signal due to **11** increases, giving an **18A**/**11** ratio of 55:45.

^{13}C NMR ($CDCl_3$, −50 °C): ∼147.6, 144.7, 138.9, 137.9 (br, C_6F_5), 135.6−124.6 (Ph), 113.2 (s, C_β, $P-C_\alpha{\equiv}C_\beta Bu^t$), 108.9 (m, br, this signal can tentatively be assigned to C_β, $-C_\alpha{\equiv}C_\beta Bu^t$), 87.18 (dm, signal poorly resolved, C_α, $-C_\alpha{\equiv}C_\beta Bu^t$), 70.5 (d, $^1J_{CP}$ = 97.1 Hz, C_α, $P-C_\alpha{\equiv}C_\beta Bu^t$), 30.6, 30.4 (s, $2C(CH_3)_3$), 29.7, 29.6 (s, br, CMe_3).

Reaction of *cis*-[Pt(C≡CBu^t)$_2$L$^2_2$] (4) with 2 Equiv of *cis*-[Pd(C_6F_5)$_2$(thf)$_2$]. The reaction of **4** (0.0152 g, 0.171 mmol) with *cis*-[Pd(C_6F_5)$_2$(thf)$_2$] (0.020 g, 0.034 mmol) in $CDCl_3$ (0.6 cm^3) was monitored by NMR spectroscopy. The dinuclear derivative **12** was observed as the only phosphorous-containing platinum complex (^{31}P and ^{1}H NMR), and no evolution of the $^{31}P\{^1H\}$ NMR spectrum was observed after 4 or 8 h. The presence of the excess of "*cis*-Pd(C_6F_5)$_2$" (∼−117.3 (F_o), −159.9

(31) Gastinger, R. G.; Anderson, B. B.; Klabunde, K. *J. Am. Chem. Soc.* **1980**, *102*, 4959.

(F_p), −163.5 (F_m)) together with the signals due to $C_6F_5-C_6F_5$ (−137.6 (m), −149.9 (t), −160.4 (m)) (60:40) are visible in the ^{19}F NMR spectra.

X-ray Crystal Structure Determinations. Suitable crystals of **10**·Me_2CO were grown by slow diffusion of *n*-hexane into a Me_2CO solution of **10**. Suitable crystals of **15A**·$0.5C_6H_{14}$·$0.45C_6H_6$ were grown by slow diffusion of *n*-hexane into a dichloromethane/benzene solution of **15A**. Suitable crystals of **16B** were grown by slow diffusion of *n*-hexane into a CH_2Cl_2 solution of **16B** at −40 °C.

Crystal data and other details of the structure analyses are presented in Table 7. Selected crystals were fixed on top of glass or quartz fibers and mounted on the diffractometers. Unit cell constants were determined from 22 accurately centered reflections with $24° < 2\theta < 26°$ for **10**·Me_2CO, 25 reflections in the range $22.2° < 2\theta < 30.9°$ for **15A**·$0.5C_6H_{14}$·$0.45C_6H_6$, and 25 reflections in the range $22.2° < 2\theta < 31.8°$ for **16B**. Data were collected by the $\omega/2\theta$ scans for **10**·Me_2CO and by ω/θ scans for **15A**·$0.5C_6H_{14}$·$0.45C_6H_6$ and **16B**. Three check reflections were measured at regular intervals, and no loss of intensity was observed in any case. The position of the heavy atoms were determined from the Patterson map. The remaining atoms were located in successive difference Fourier syntheses. H atoms were added at calculated positions (C−H = 0.96 Å) with an isotropic displacement parameter assigned 1.2 times (for the phenyl groups) or 1.5 times (for the methyl groups) that of the corresponding C atom. For **10**·Me_2CO, a molecule of insterstitial acetone was found and refined at full occupancy with anisotropic thermal parameters, and no H atoms were added to the acetone molecule. For **15A**·$0.5C_6H_{14}$·$0.45C_6H_6$, whereas the positions and thermal parameters of the atoms of the platinum complex were found and refined without difficulty, the electron density corresponding to the solvent molecule atoms was very diffuse. We tried several models and found that the one which gave best results was the presence of one molecule of *n*-hexane with an occupancy of 0.5, one molecule of benzene with an occupancy of 0.3, and one-half of a molecule of benzene lying around an inversion center whose three carbon atoms had occupancy 0.3. Both solvents had been used in the obtention of the crystals. The interatomic distances and angles were constrained to idealized geometries, and the anisotropic thermal parameters of the carbon atoms of each molecule were constrained to be the same. No attempts to include the solvent hydrogen atoms were made. For **10**·Me_2CO and **16B**, no residual peaks higher than 1 e/Å^3 remained in the final density map. For **15A**·$0.5C_6H_{14}$·$0.45C_6H_6$, the final difference electron density maps showed eight peaks above 1 e Å^{-3} (1.08−1.02; largest diff hole −0.76), all of them located in the solvent area. All calculations were carried out using the program SHELXL-93.[32]

Acknowledgment. We thank the Dirección General de Investigación Científica y Técnica (Spain) (Project Nos. PB 95-0003-C02-01-02 and PB 95-0792) for financial support. E. Lalinde and M. T. Moreno thank the University of La Rioja (Spain) for financial support.

Supporting Information Available: Tables of full atomic positional and equivalent isotropic displacement parameters, anisotropic displacement parameters, full bond distances and bond angles, and hydrogen coordinates and isotropic displacement parameters for the crystal structures of complexes **10**, **15A**, and **16B** (41 pages). Ordering information is given on any current masthead page.

OM970663Y

(32) Sheldrick, G. M. *SHELXL-93, a program for crystal structure determination*; University of Göttingen: Göttingen, Germany, 1993.